END
DATE
FILMED
8

EOARD-TR-87-09

②

Grant Number: AFOSR-84-0338

HOT CORROSION IN GAS TURBINES : A NEW, UNIQUE AND INFORMATIVE TECHNIQUE IS EASE.

Trevor R. Griffiths
Department of Inorganic and Structural Chemistry
The University of Leeds
LEEDS
West Yorkshire LS2 9JT
United Kingdom

20 May 1987

Final Report, 31 July 1984 - 1 December 1986.

Prepared for

87 10 ?? 012

REPORT DOCUMENTATION PAGE

1a REPORT SECURITY CLASSIFICATION Unclassified		1b. RESTRICTIVE MARKINGS		
2a SECURITY CLASSIFICATION AUTHORITY		3. DISTRIBUTION/AVAILABILITY OF REPORT Approved for public release; Distribution unlimited		
2b DECLASSIFICATION/DOWNGRADING SCHEDULE				
4. PERFORMING ORGANIZATION REPORT NUMBER(S)		5. MONITORING ORGANIZATION REPORT NUMBER(S) EOARD·TR·87 09		
6a NAME OF PERFORMING ORGANIZATION The University of Leeds	6b OFFICE SYMBOL (If applicable)	7a. NAME OF MONITORING ORGANIZATION European Office of Aerospace Research and Development		
6c. ADDRESS (City, State, and ZIP Code) Department of Inorganic and Structural Chemistry Leeds LS2 9JT, United Kingdom		7b ADDRESS (City, State, and ZIP Code) Box 14 FPO New York 09510-0200		
8a. NAME OF FUNDING/SPONSORING ORGANIZATION European Office of Aerospace Research & Development	8b OFFICE SYMBOL (If applicable) LRP	9. PROCUREMENT INSTRUMENT IDENTIFICATION NUMBER AFOSR 84-0338		
8c. ADDRESS (City, State, and ZIP Code) Box 14 FPO New York 09510-0200		10 SOURCE OF FUNDING NUMBERS		

PROGRAM ELEMENT NO 61102F	PROJECT NO 2301	TASK NO D1	WORK UNIT ACCESSION NO

11. TITLE (Include Security Classification)

HOT CORROSION IN GAS TURBINES: A NEW, UNIQUE AND INFORMATIVE TECHNIQUE IS EASE

12. PERSONAL AUTHOR(S) Dr. Trevor R. Griffiths

13a. TYPE OF REPORT Final Scientific	13b TIME COVERED FROM 31Jul84 TO 1 Dec86	14 DATE OF REPORT (Year, Month, Day) 1987 May 20	15 PAGE COUNT 7&

16. SUPPLEMENTARY NOTATION

17	COSATI CODES		18 SUBJECT TERMS (Continue on reverse if necessary and identify by block number)
FIELD	GROUP	SUB-GROUP	EASE (electronic absorption spectroscopy experiments),gas turbines, advanced turbine materials, aerospace applications, molten sulfates, hot corrosion, spectroscopy, furnaces,chloride corrosion, crucible tests, fiber optics.

19 ABSTRACT (Continue on reverse if necessary and identify by block number) The hot corrosion of advanced turbine materials used in aerospace applications may now be studied successfully with EASE (Electronic Absorption Spectroscopy Experiments). This technique permits the continuous monitoring of the dissolution of corrosion products into molten sulphate deposits under conditions which replicate effectively operating conditions. The EASE technique was originally developed for studying hot corrosion on superheater tubes, and this preliminary study has developed and extended it to turbine materials, where the effects of thermal cycling and chloride addition can be followed. The report details the spectroscopic studies made and how rates are obtained from spectra; the design and testing of thermal gradient furnaces; and some crucible and spectroscopic studies of IN 738 in sulphate + chloride melts. A recently marketed American Fiber optic spectrophotometer could be modified to enhance EASE studies and make in situ studies of operating turbines.

20. DISTRIBUTION/AVAILABILITY OF ABSTRACT ☐ UNCLASSIFIED/UNLIMITED ☒ SAME AS RPT ☒ DTIC USERS	21 ABSTRACT SECURITY CLASSIFICATION Unclassified		
22a. NAME OF RESPONSIBLE INDIVIDUAL Lt Col LaRell K. Smith	22b TELEPHONE (Include Area Code) (44 1) 409-4505	22c OFFICE SYMBOL EOARD/LRP	

DD FORM 1473, 84 MAR   83 APR edition may be used until exhausted
All other editions are obsolete

EOARD-TR-87-09

This report has been reviewed by the EOARD Information Office and is releasable to the National Technical Information Service (NTIS). At NTIS it will be releasable to the general public, including foreign nations.

This technical report has been reviewed and is approved for publication.

LARELL K. SMITH, Lt Col, USAF
Chief, Physical Chemistry/Materials

ROBERT C. WINN, Lt Colonel, USAF
Chief Scientist

Preface

The work reported here has been associated with studies also
using and developing the EASE technique (Electronic Absorption
Spectroscopy Experiments) on the related topic of hot corrosion
by molten salt deposits, but occurring on superheater and reheater
tubes in fossil fuel fired power generation plant. Naturally,
at times, the findings of Dr. Hubbard, the Experimental Officer
for this project, were applicable both to this project and super-
heater corrosion, and *vice versa*. The contributions and co-
operation of research students Keith King and Susan Marchant are
gratefully acknowledged, as are their co-sponsors, the Science
and Engineering Research Council (SERC) and the Central Electricity
Generating Board (CEGB), N.E. Region, and we thank the latter for
the use of their in-house reports.

- 1 -

TABLE OF CONTENTS

1. PURPOSE AND SCOPE

1.1. Background

The hot corrosion of advanced turbine materials used in
aerospace applications may now be studied with EASE. The acronym
EASE stands for Electronic Absorption Spectroscopy Experiments, and
the technique was originally developed at Leeds University to
investigate the hot corrosion occurring on superheater and reheater
tubes in fossil fuel fired power generation plant. Such corrosion
is brought about by molten sulphate deposits similar to those
occuring in gas turbines. The EASE technique has many features and
advantages, and is unique in that in principle it permits the cont-
inuous monitoring of the dissolution of corrosion products into the
molten sulphate under heat flux conditions which replicate effectively
in-plant conditions. It was therefore of interest and appropriate
to continue its development and apply it to hot corrosion in gas
turbines, especially that by molten sulphates containing added
chloride.

The immediate objectives were to establish the necessary back-
ground and practical knowledge and extensions to the EASE apparatus
and technique that would be necessary so that new information would
be obtained on advanced aerospace materials, and this report
describes our successes and how most of this has been achieved. The
long term general objectives are (1) to adapt, streamline and
partially automate the EASE technique to study hot corrosion in gas
turbines; (2) to acquire data necessary regarding superalloys and
the like by crucible tests (analysing the melt), combined with a
fundamental study of the chemistry of niobium, tantalum, molybdenum
and tungsten in molten sulphate (and with added chloride) using
electronic absorption spectroscopy, since this is lacking in the
literature; and (3) using EASE, and replicating closely as many
operational conditions as possible, obtain new information regarding
corrosion rates, mechanisms and models for advanced aerospace
materials.

A hope long harboured has been that spectroscopic
measurements could be made rapidly in normally inaccessible places
using fibre optics as light guides. After the practical side of
this report was complete a portable commercial instrument, termed
a Guided Wave Analyser, appeared on the European market a few
months ago. It is American made (and had been released on the
American market a year earlier) and is fully automated and computerised.
The Principal Investigator has had one demonstrated in his laboratory,
and concludes that such instruments are the new generation of versatile
spectrophotometers. With certain modifications they could be adapted
to enhance considerably data collection and manipulation during EASE
measurements. In principle, with some cooling of the fibre tip, and
using a strobe light source, the spectra of molten sulphate deposits
on individual blades in an operating gas turbine could be measured
and monitored. Additional comments on future work using the present
system are given on pages 39-41.

1.2. Operational Procedures

The project was seen as taking place on three levels; an
efficiently working base system; melding into current hot corrosion
research; and new research, particularly the testing of speculations.

a. Efficiently working base system.

With an efficient system, systematic investigations can be
made quickly and reliably, and speculative investigations can be
followed up effectively. Over the years various research students
had contributed in their individual ways to our understanding of
molten salt spectroscopy, but it was now appropriate, having defined
objectives, to systematize and regularize the base procedures of
servicing, equipment replacement, stock-taking, calibration of
instruments, (spectrophotometers and furnaces in particular), and
compilations of basic data.

b. Integration with current hot corrosion research.

In our development of molten salt spectroscopy, and more recently

its application to hot corrosion, various research students had produced a variety of useful practical procedures and computer programs. It was now appropriate, and especially for this project, to consolidate, systematize and establish the reliability and domain of these procedures and techniques. Further, theoretical considerations then are needed, to identify possible sources of ambiguities and errors, to build confidence into simple systems, allow extension to complex systems, and formulate standard procedures. The various computing programs and approaches, developed in the past using different languages required integration into a uniform access and implementation procedure, together with the setting up of a spectral database. The opportunity was also taken to start transferring literature references and important past observations into computerised notebook form.

This project also prompted cross-correlation with other techniques employed in the Chemistry and Applied Science departments of the University, particularly X-ray studies, electron microscopy, and standard metallurgical preparative and testing procedures.

c. New research, and the testing of ideas.

In the testing of the hot corrosion of superalloys it is necessary to make crucible and spectroscopic (EASE) investigations under relevant conditions while gleaning new data from analysis of the molten salt solutions. Results known from metallurgical investigations must be carefully married with chemical findings, making due allowance for different experimental conditions. Possible ways of using the EASE technique to derive, for example, diffusion and Soret coefficients for transition metal ions in molten salts are potentially available, employing realistic operating conditions. Also, new computing programs can be developed, tested and produced in support of the above.

2. SPECTROSCOPIC STUDIES

2.1. Introduction

There are relatively few reports in the literature of the spectra of transition metal ions in sulphate melts, and only the earlier

work by us for the spectra of such ions in aluminium-containing
sulphate melts (1). The corresponding spectra in chloride systems
(including those containing $AlCl_3$) are more widely reported. There
are, however, no reports for mixed sulphate-chloride melts.

Our use of aluminium-containing sulphate melts, specifically
(Na, K, Al)SO_4, have cation mole ratios, respectively, of 42.5:42.5:15,
stems from our original EASE technique studies relating to hot
corrosion in coal-fired steam-generating plant (2,3). Although the
major cations found from analysis of deposits were sodium and
potassium, the (Na,K)SO_4 eutectic mixture melted at around 800°C,
well above the known melting point of the sulphate deposit on super-
heater tubes of around 550°C. Previous crucible tests achieved this
lower liquidus temperature by using the ternary eutectic (Li,Na,K)SO_4,
but here the cation mole percent of lithium is 78. Although lithium
is a minor constituent of superheater deposits, the CEGB had for many
years used this eutectic mixture to their satisfaction : we opted to
search for a ternary sulphate mixture employing one of the next most
abundant elements found in deposits after sodium and potassium (1),
and which would need to be present in smaller amounts than these
other two cations. Preliminary comparative corrosion rate tests have
indicated that our aluminium-containing melts were approximately
twice as corrosive as the lithium -containing eutectic.

When considering the application of our EASE technique to hot
corrosion in gas turbines we were unhappy with the common North
American concept that the melt involved in low temperature hot
corrosion was largely the sodium sulphate-cobalt sulphate eutectic.
This latter was based on phase diagram considerations, since
insufficient sulphate deposits for analysis are found on, (or allowed
to remain on), aircraft gas turbine engines or burner-rig assemblies.

(1). T.R. Griffiths and K. King, J. Chem. Soc., Faraday Trans. 1, 1981,
      77, 2763.

(2). T.R. Griffiths, K. King and D. Mortimer, High Temp. Technology,
      1982, 1, 43.

(3). T.R. Griffiths, K. King and D. Mortimer, Power Ind. Res., 1982, 2, 79.

Our enquiries with European turbine specialists, and
general reading, showed a preference for an alternative explanation,
but no universal (or Continentally acceptable) alternative was
advanced: the concept that molten sodium sulphate would be deposited
(mp 884°C), and that this would oxidise the cobalt in the superalloy,
and take it into solution was not considered likely or feasible. We
therefore considered the situation and favoured investigating the
behaviour of synthetic sea-salt mixed with varying amounts of sea-salt
sulphate, i.e., a sulphate mixture containing the relative amounts of
the cations within synthetic sea-salt. Unfortunately the time-scale
of this project did not permit us to commence studies of and within
these mixtures, and we deemed it more profitable to use, for the
moment, the lithium-containing and the aluminium-containing sulphates,
to link in better with our previous and existing work. However, we
do consider that a major part of future studies should be on the
behaviour of metals, alloys and coated alloys in sea-salt sulphate
and chloride melts.

Before the behaviour of alloys in molten sulphates can be
studied spectroscopically, it is necessary to know the main features
of the spectra of ions of the individual component elements in these
melts, and the interaction of each metallic element with these melts.
Our studies on nickel were essentially complete and have been
published (3), but work on chromium and iron were incomplete, and
have been continued in this project and are therefore here reported.

2.2. Chromium(III) and Iron(III) in Melts.

The chromium(III) spectra in (Li, Na, K)SO_4 at 600°C has been
recorded by Johnson et al. (4). They identified an octahedral species
which they proposed as $[Cr(SO_4)_3]^{3-}$, with three bidentate sulphate
ligands. The Cr(III) spectrum in (Li, K)Cl eutectic was recorded by
Harrington and Sundheim (5), who noted slight changes upon increasing

---

(4). K.E. Johnson, R. Palmer and T.S. Piper, Spectrochim. Acta, 1965,
   21, 1697.

(5). G. Harrington and B.R. Sundheim, Ann. N.Y. Acad. Sci., 1960, 79, 950.

the temperature from 392 to 444°C. The $[CrCl_6]^{3-}$ species was proposed, and the observed changes attributed to thermal perturbations. Gruen and McBeth (6) also examined this system, and extended the temperature range to 1000°C. Even at the highest temperature the spectrum could still be interpreted on the basis of $[CrCl_6]^{3-}$ octahedra, with no indication of an octahedral-tetrahedral equilibrium, (which is a common feature of chloride melts containing nickel(II)).

Iron(III) is $\underline{d}^5$ ion and thus $\underline{d}$-$\underline{d}$ transitions are both Laporte and spin-forbidden. As a consequence, the bands are very weak, and their observation is further limited by a very strong charge transfer edge, which dominates the iron(III) spectrum in molten systems. Harrington and Sundheim (5) obtained the spectrum in (Li,K)Cl eutectic, finding a strongly absorbing shoulder below 400 nm on the edge of a band which rose sharply around 250 nm. Increasing the temperature from 373 to 434°C caused the shoulder to diminish. Comparison of the spectra with others of iron(III) in a variety of non-aqueous solvents led the authors to propose a tetrahedral $[FeCl_4]^-$ species. *Silcox and Haendler (7) recorded* the ultraviolet spectrum of iron(III) in the (Na, K, Mg)Cl eutectic at 430°C, and again a rising absorption edge was found, but this time containing possible indications of weak bands. No identification of the iron species was attempted.

We have published a preliminary report (8) on the spectrum of iron(III) in chloride and, for the first time, sulphate melts in which we identified many of the weak bands, and concluded that tetrahedral complex ions were formed in both chloride and sulphate melts.

(6). D.M. Gruen and R.L. McBeth, Paper for the Seventh International Conference on Coordination Chemistry, Stockholm (June 1962).

(7). N.W. Silcox and H.M. Haendler, J. Phys. Chem., 1960, 64, 303.

(8). T.R. Griffitns and K. King, Chem. Comm., 1981, 518.

3.   COORDINATION COMPLEXES IN MOLTEN SALTS

The assertion that discrete co-ordination complexes exist in molten salts
at high temperatures has at times been questioned. The alternative
view (9) is that the metal ion is merely at a centre having, say,
basically octahedral or tetrahedral symmetry, and that the lifetime
of a given anion contiguous to the metal is very short, and thus no
bonding between metal and ligand can occur. While this may be the
case at temperatures approaching 1000°C, there is ample evidence
for the existence of discrete complexes at temperatures pertinent
to this project. This evidence includes the effect of very small
additions on nickel(II) spectra in nitrate melts (10). Such
additions produce large changes in the spectra, which would not be
possible unless discrete chloride-containing complexes were formed.
Equally strong evidence for complex formation arises from the
appearance of identical spectra in molten salts and in appropriate
non-aqueous solvents, where discrete complexes are known to exist.
We therefore conclude that for this study our spectra are to be
interpreted in terms of complex ions, but for future work at
higher temperatures, the existence of cations at the centres of
various anion site symmetries will have to be assessed as possible
contributors to the overall understanding.

3.1.   Spectra obtained using Sulphate Melts with Added Chloride

Typical spectra for Ni(II), Cr(III) and Fe(III) in molten
(Na, K, Al)SO_4 have been published and briefly described (1) :
spectra in mixed sulphate with chloride melts have not previously
been reported.

It was initially found that it was not possible to investigate
the effect of temperature upon a melt of given chloride content.

---

(9).   J. Brynestad, C.R. Boston and G.P. Smith, J. Chem. Phys.,
       1967, 47, 3179.

(10). T.R. Griffiths and P.J. Potts, Inorg. Chem., 1975, 14, 1039.

Al_2Cl_6 is slowly lost from these melts, and thus significant
melt composition changes would have occurred in the time required
for thermal equilibration at each temperature. The best procedure
was therefore to keep the melt temperature constant and add the
chloride in approximately 5 mol anion percent increments. At the
end of each run the chloride content of a solidified melt sample
was analysed. In all cases the chloride content was within ± 2
mol anion percent of the expected value.

It was also found that chloride additions enhanced the
decomposition of the melt, as evidence by the formation of a
precipitate. Thus, at the highest temperature (730°C), chloride
additions were limited to 45 mol anion percent for chromium and
iron, but 35 mol anion percent for nickel, since a larger scan
range was required for this ion, and thus each spectrum took
longer to record. A water-insoluble white residue was isolated
from melt samples in which decomposition had taken place, and was
shown to be Al_2O_3 by micro-analysis.

3.2. Nickel(II) in Sulphate Melts with Added Chloride.

The variation of the nickel(II) spectrum with chloride content
from 0 to 35 mol anion percent was recorded over the temperature
range 587-720°C. At 587°C the system was very near its melting point
and too opaque for recording spectra at chloride content below 15 mol
anion percent. The variation with chloride content at 600 and 720°C
is shown in Figs. 1 and 2, respectively.

The spectrum of nickel(II) in the pure ternary sulphate melt,
(Na, K, Al)SO_4, is similar to that in the (Li, Na, K)SO_4 melt (11),
except that the shoulder on the low energy side of the main band is
much more pronounced in the aluminium-containing melt. The effect
of increasing the temperature is to shift the whole spectrum to

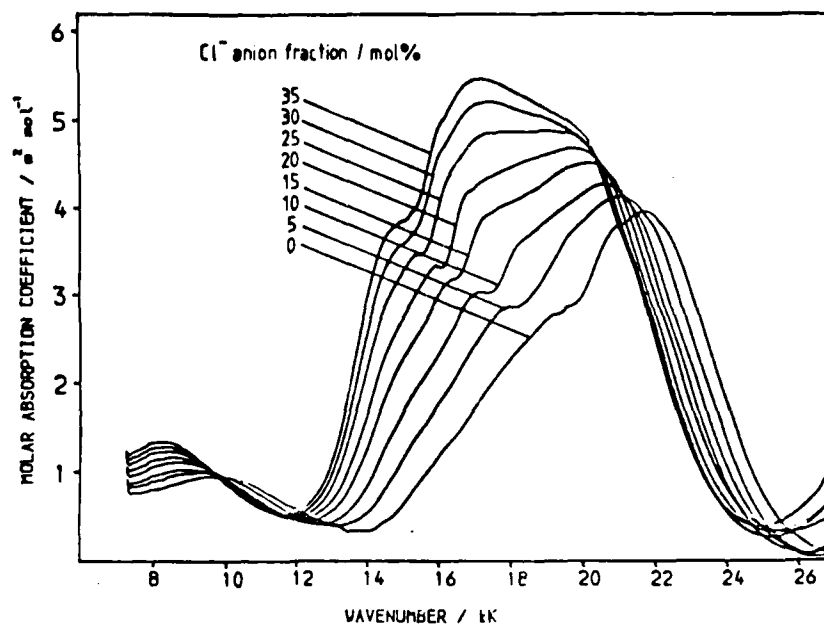(11). K.E. Johnson and T.S. Piper, Discuss. Faraday Soc., 1961, 32, 32.

Figure 1   Variation of nickel(II) spectrum in (Na,K,Al)(SO₄,Cl) with chloride content.
at 600°C (49 point smoothing fifth order polynomial).
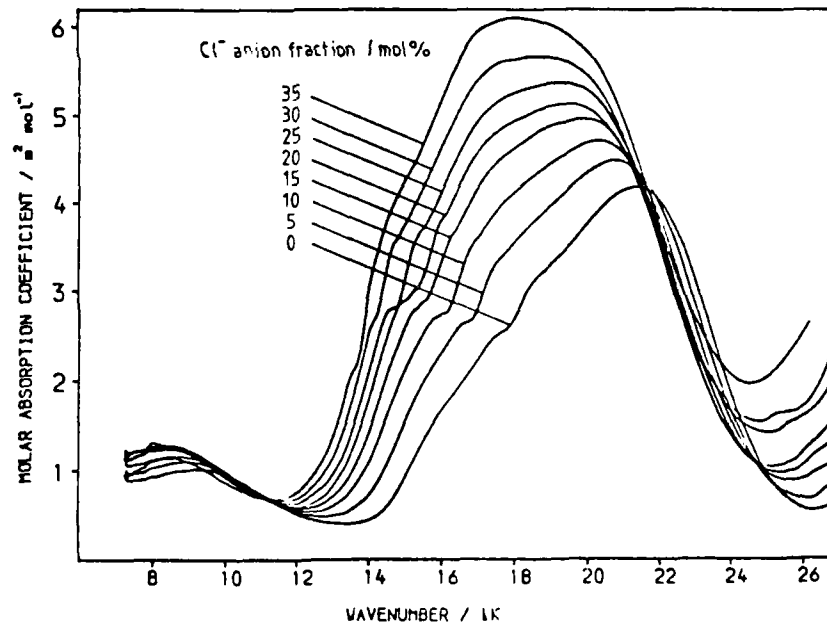
Figure 2   Variation of nickel(II) spectrum in (Na,K,Al)(SO₄,Cl) with chloride
content, at 720°C (49 point smoothing, fifth order polynomial).

slightly lower energy, and to introduce a second shoulder on the low energy side of the main band. The progressive broadening of bands with increasing temperature tended to mask these effects.

The addition of chloride ions has a dramatic effect on the spectra at all temperatures. As the chloride content is increased, the original main band diminishes and the spectra becomes dominated by bands emerging at lower energies. The addition of chloride is also accompanied by the establishment of a number of isosbestic points at approximately 10,000, 12,000, 20,000 and 25,000 cm^{-1}. However, not all the curves pass through these points and there is an apparent improvement in the convergence with increasing temperature.

The occurrence of isosbestic points has often been taken as an indication of a two species equilibrium. A more detailed analysis is given in Section 3.5.

To establish the effect of complete replacement of sulphate by chloride in the melt, the spectrum of nickel(II) chloride in the (Na, K, Al)Cl melt, having the same cation ratios as the eutectic (Na, K, Al)SO_4, was recorded at 692°C. This is shown in Fig. 3, along with the spectra for chloride additions to the sulphate melt at that temperature. The spectrum in (Na, K, Al)Cl is very similar to that reported by Smith (12) for nickel(II) in fused CsCl at 800°C.

a. Higher Derivative Analysis

Both second and fourth derivative analyses were performed, and good agreement between the two was found. Simultaneous smoothing and differentiation was utilised (13), equivalent to a 49 point different- iation of a 49 point smoothed spectrum, fitting a fifth order polynomal. The uncertainties in the energies of the bands obtained were estimated at ± 200 cm^{-1}.

(12). G.P. Smith, in 'Molten Salt Chemistry', Ed. M. Blander, Wiley and Sons (1964).

(13). T.R. Griffiths, K. King, H.V. St.A. Hubbard, M-J Schwing-Weill and J. Meullemeestre, Anal. Chim. Acta, 1982, 143, 163.
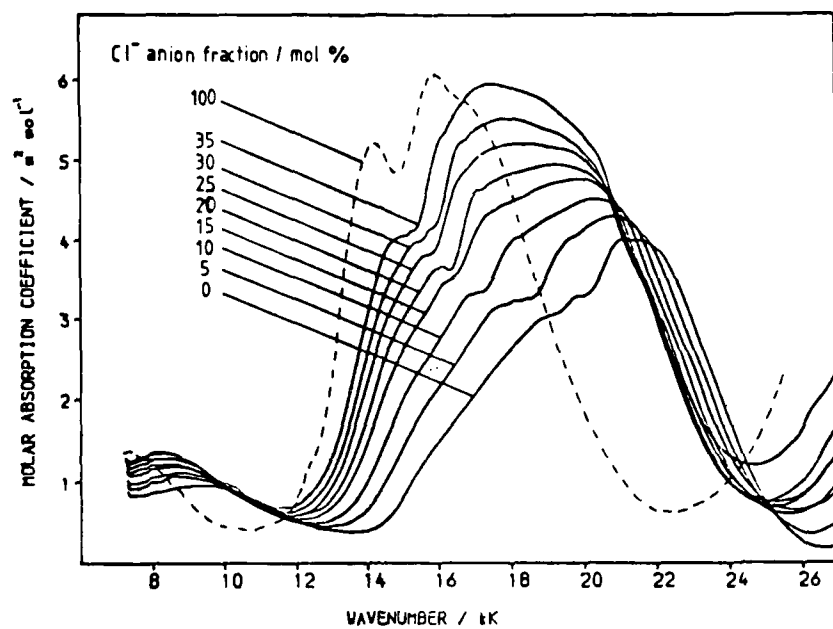
Figure 3   Variation of nickel(II) spectrum in (Na,K,Al)(SO$_4$,Cl) with chloride content,
and spectrum in (Na,K,Al)Cl (dashed line), at 692°C (49 point smoothing,
fifth order polynomial).

For the spectra in the (Na, K, Al)(SO$_4$, Cl) system up to
six bands (labelled A-F) were identified, although all of them
were not always present. Representative second and fourth derivatives
are shown in Fig. 4. The variation of the energies of the resolved
bands with chloride content, at the six temperatures investigated,
is shown in Fig. 5.

A similar analysis of the nickel(II) spectrum in (Na, K, Al)Cl
yielded four main bands at 17,500, 15,800, 14,300 and 13,400 cm^{-1},
and these may be associated with the bands C-F, respectively, above.

b. Discussion

In the spectrochemical series for molten salts reported by
Johnson (14), sulphate appears directly above chloride. A shift to
lower energy is therefore expected as sulphate ligands are replaced
by chloride in the nickel coordination sphere. The interpretation of
the mixed sulphate-chloride spectra is aided by the results from the
analysis of nickel(II) in (Na, K, Al)Cl, and so this will be considered
first.

The similarity of the nickel(II) spectra in fused CsCl and in
a crystal of Cs$_2$ZnCl$_4$ doped with Cs$_2$NiCl$_4$, in which nickel ions are
known to be tetrahedrally coordinated, led Smith (12) to conclude that
nickel complexes of T$_d$ symmetry were present in the CsCl melt. The
same conclusion may be drawn here, regarding nickel(II) in the fused
(Na, K, Al)Cl melt. Assuming a Dq value of 370 cm^{-1} for the NiCl$_4^{2-}$
complex (12), bands C, D and E may be assigned to the ^{3}T$_1$(F) $\rightarrow$ ^{3}T$_1$(P)
transition. This triplet state is split into three distinct bands by
spin-orbit coupling (12). Band F, which is much less pronounced than
the rest, may be assigned to the spin-forbidden transition ^{3}T$_1$(F) $\rightarrow$
^{1}E(D) or ^{1}T$_2$(D) : subsequent more detailed work may reveal this band to
be made up of two bands close together.

Considering now the mixed sulphate-chloride spectra it is
clear that tetrahedral nickel species are present in these melts.

---

(14). K.E. Johnson, Electrochim. Acta, 1966, 11, 129.
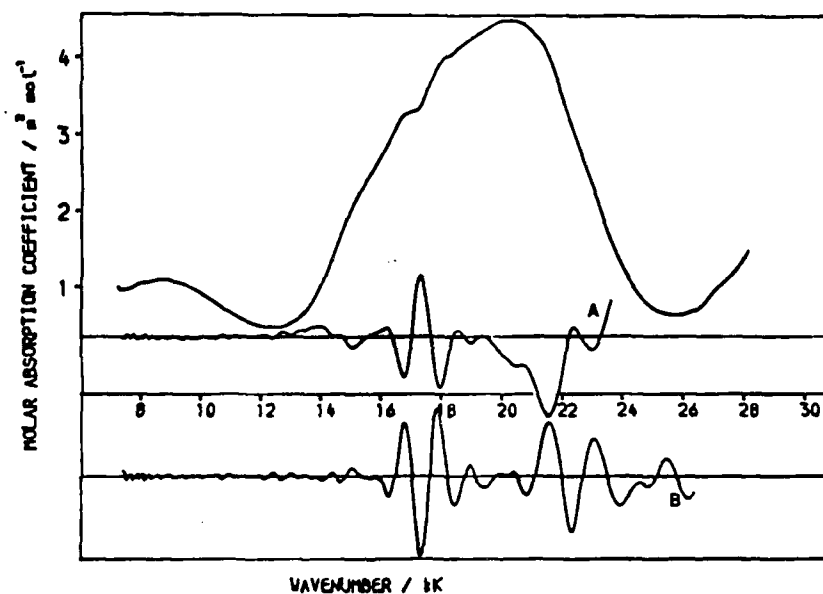
Figure 4   Spectrum of nickel(II) in (Na.K.Al)(SO$_4$.Cl). containing 10 mol anion %
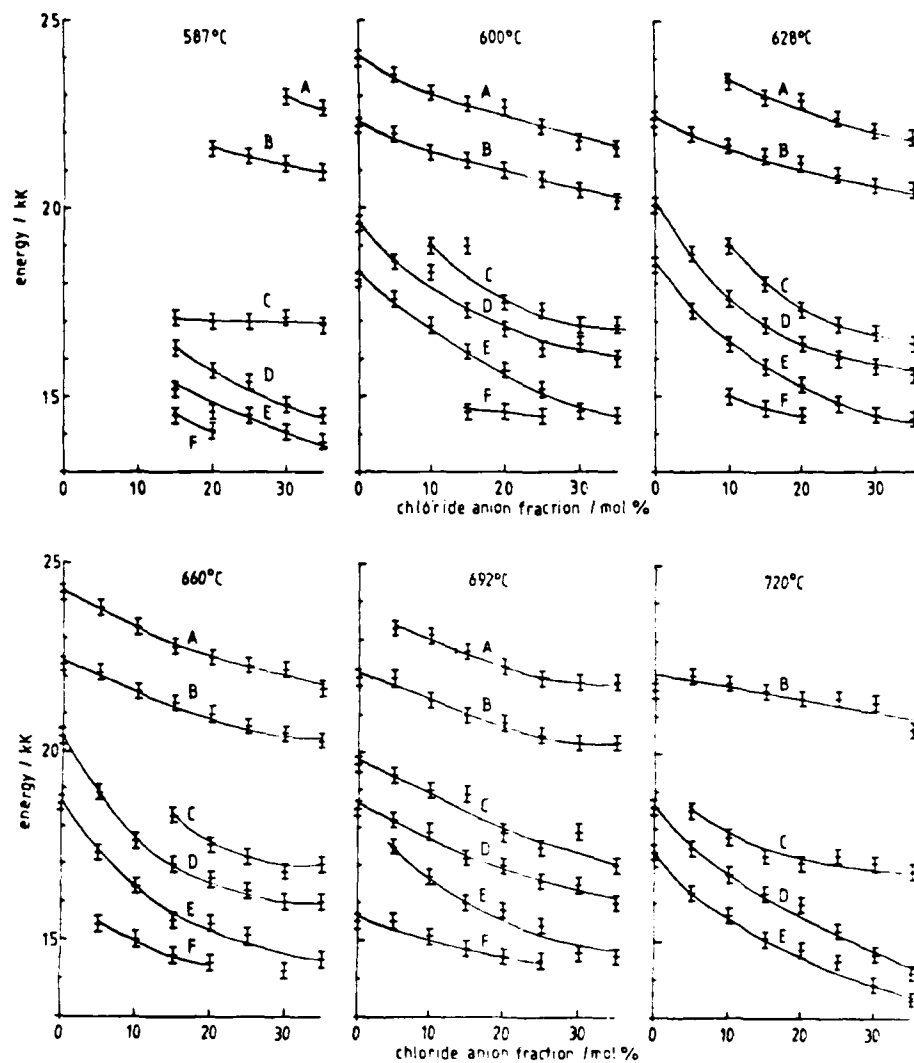chloride at 692°C.   A. second derivative: B. fourth derivative.

- 14 -

Figure 5   Variation in energies of resolved bands of the nickel(II) spectrum in (Na K Al)(SO₄ Cl) with chloride content at 587, 600, 628, 660, 692 and 720°C.

- 15 -

Bands A and B may be assigned to transitions in an octahedral
complex : band B is the main transition $^3A_{2g} \rightarrow {}^3T_{1g}(P)$, and band
B may be a spin-forbidden transition to the $^1A_{1g}$ or $^1T_{1g}$ state,
from the ^1G free ion term, and again more work is merited.

There are therefore O_h and T_d nickel species in the pure
(Na, K, Al)SO_4 melt. The octahedral complex is clearly
$[Ni(SO_4)_3]^{4-}$, (strictly, it has D_3 symmetry, but the crystal field
of the metal ion may be taken as O_h), with three bidentate sulphate
ligands (11). The tetrahedral species, identified by two of the
three components of the transition $^3T_1(F) \rightarrow {}^3T_1(P)$, is not so well
defined, the choice being between mono- and bidentate sulphate
ligands. The former is favoured since there is now a greater
distance between pairs of sites to be bridged by a bidentate ligand,
and also because of the lower coordination number, so that four
sulphates could be accommodated around the nickel atom, whereas six
(to form octahedral $[Ni(SO_4)_6]^{10-}$) might not. It is thus here
concluded that the tetrahedral species is $[Ni(SO_4)_4]^{6-}$.

The effect of temperature upon the spectrum is to shift the
band to lower energy, and make the components due to the tetrahedral
species more prominent. This indicates that higher temperatures
favour the formation of tetrahedral nickel. Similar results have been
obtained in chloride melts (15). At the highest temperature, 720°C, the
spin-forbidden bands A and F are no longer detected (Fig. 5). This
results from the thermal broadening of the relatively strong spin-
allowed bands.

The addition of chloride to the (Na, K, Al)SO_4 melt has a
markedly different effect upon the tetrahedral bands (C-F),
compared with the octahedral bands A and B. Both sets are shifted
progressively, but the tetrahedral bands to a much greater extent.
The shift is due to the admission of chloride ions into the

---

(15). C.A. Angell and D.M. Gruen, J. Phys. Chem., 1966, 70, 1601.

coordination sphere of the nickel. But for the tetrahedral bands
the replacement of, say, one oxygen atom (of a sulphate ligand) by
a chloride ion has a greater effect on the crystal field splitting
in the tetrahedral complex than in the octahedral.

3.3. Chromium(III) in Sulphate Melts with Added Chloride.

The effect of chlorides on the spectrum of chromium(III) in
(Na, K, Al)SO$_4$ is comparatively small and virtually temperature
independent in the range examined 610 - 730°C. The variation is
shown, at 610°C, in Fig. 6 and at 692°C, in Fig. 7. The spectrum
of Cr(III) in the (Na, K, Al)Cl melt, at 692°C, is also shown in
Fig. 7.

The effect of increasing temperature on the spectrum in
(Na, K, Al)SO$_4$ is to produce a very slight shift to lower energy.
Additionally, the doublet at 14,000 cm^{-1} (Fig. 6) becomes less
pronounced : this latter effect may be attributed to thermal
broadening.

Chloride additions also cause a shift to lower energy, but
of greater magnitude than that due to increasing temperature. The
effect on the smaller band is interesting in that chloride addition
appears to increase the intensity of the lower energy component of
the doublet which comprises this band.

In the (Na, K, Al)Cl melt the Cr(III) spectrum is at lower
energy than when recorded in the mixed sulphate-chloride system.
The bands are also sharper and more intense.

Chromium(III) complexes slowly decomposed in the pure
(Na, K, Al)SO$_4$ melt, and in melts with added chloride, but only
when the melt temperature was above about 700°C. Here small
spectral changes could be detected only after several hours, and
ultimately a green precipitate formed in the melt, identified as
Cr$_2$O$_3$ by elemental analysis. Solutions around 600°C were stable
for at least 80 hours.
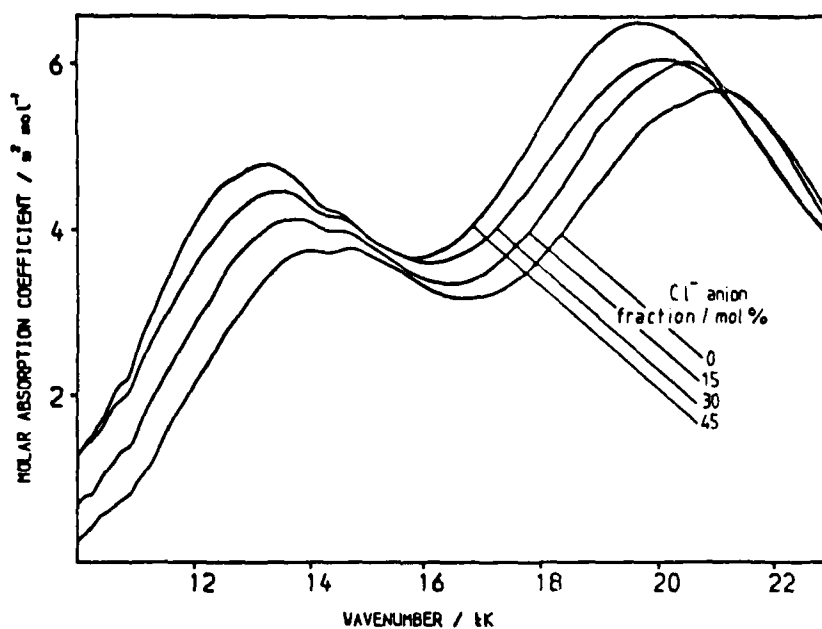
Figure 6   Variation of chromium(III) spectrum in (Na,K,Al)(SO₄ Cl) with chloride content at 610°C (47 point smoothing, fifth order polynomial).
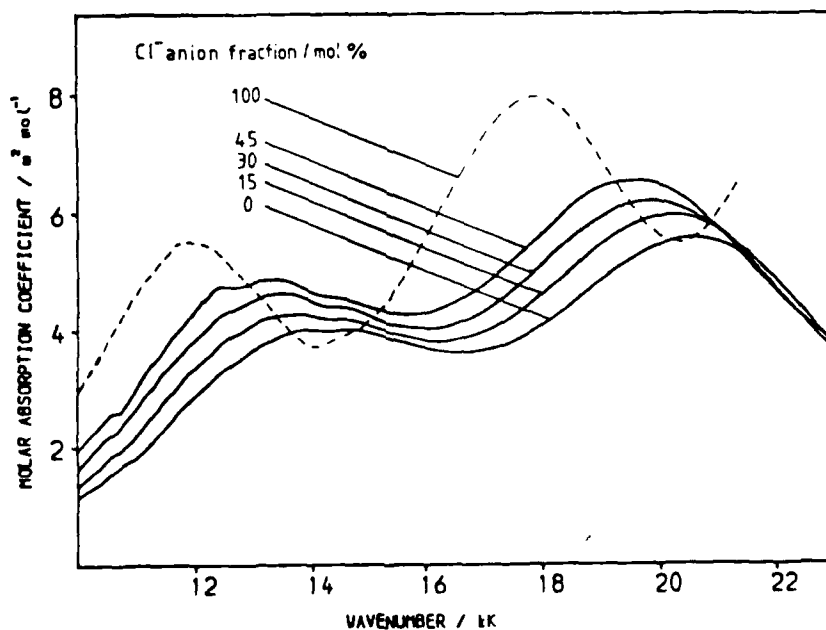
Figure 7   Variation of chromium(III) spectrum in (Na.K.Al)(SO₄.Cl) with chloride content and spectrum in (Na.K.Al)Cl (dashed line). at 696°C (47 point smoothing. fifth order polynomial).

a. Higher derivative analysis

The analysis performed is equivalent to a 47 point different-iation of a 47 point smoothed spectrum, with a fifth order polynomial. A typical result is shown in Fig. 8. The bands obtained were closely spaced and therefore not always resolved by the second derivative. However, in cases where resolution was possible, good agreement between second and fourth derivative spectra was obtained, and where a band was not resolved in the second derivative, the value obtained from the fourth derivative alone was used.

Up to ten bands (designated G-P) were obtained, and the variation of their energies with chloride content is shown in Fig. 9. Components G-I occur in the main band of the spectrum, while the smaller band comprises N-P. The remaining components, J-M, are in the region between these two bands. For the spectrum in the (Na, K, Al)Cl melt, the bands are as follows (in cm^{-1}) : G, 18,400; H, 17,600; I, 16,700; J, not observed; K, 16,000; L, 15,200; M, 14,400; N, 13,600; O, 12,800; and P, 11,700.

b. Discussion

The chromium(III) ion is highly stabilised on octahedral coordination, and $[Cr(SO_4)_3]^{3-}$ species are therefore present in the (Na, K, Al)SO_4 melt. The two main bands in the spectra may therefore be assigned to the transitions $^4A_2 \rightarrow {}^4T_{2g}(F)$ and $^4A_2 \rightarrow {}^4T_{1g}(F)$. A third band, at higher energy, due to the transition $^4A_2 \rightarrow {}^4T_{1g}(P)$, is in this case masked by the charge transfer absorption edge. The ten resolved component bands may now be assigned.

Bands G-I are the three components of the triplet transition $^4A_2 \rightarrow {}^4T_{1g}(F)$, and N-P the corresponding bands for the $^4A_2 \rightarrow {}^4T_{2g}(F)$ transition. The remaining four bands, J-M, may be assigned to four of the possible five components of the spin-forbidden transitions $^4A_2 \rightarrow {}^2T_1(G)$ and $^2E(G)$. These bands are therefore seldom detected on normally recorded spectra of octahedral Cr(III) complexes.
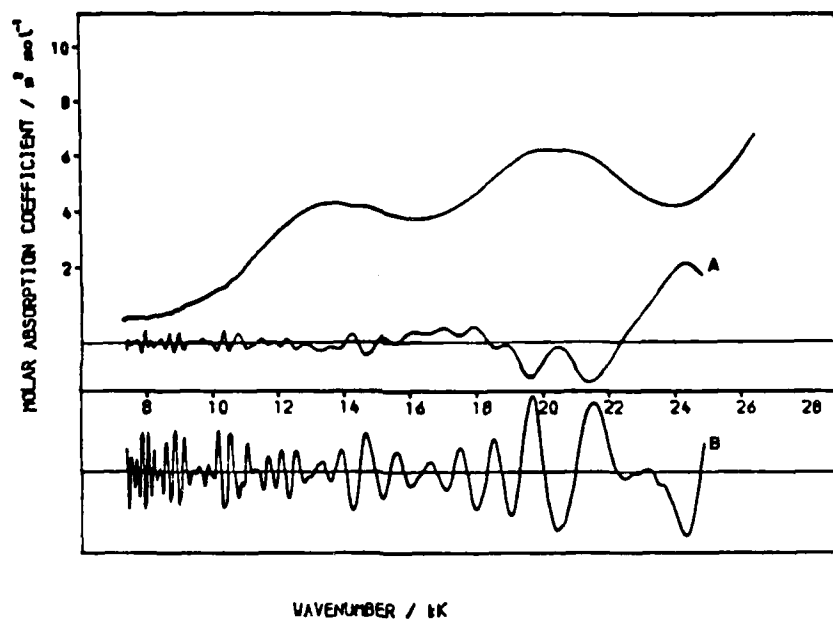
Figure 8   Spectrum of chromium(III) in (Na,K,Al)(SO$_4$,Cl), containing 20 mol anion %
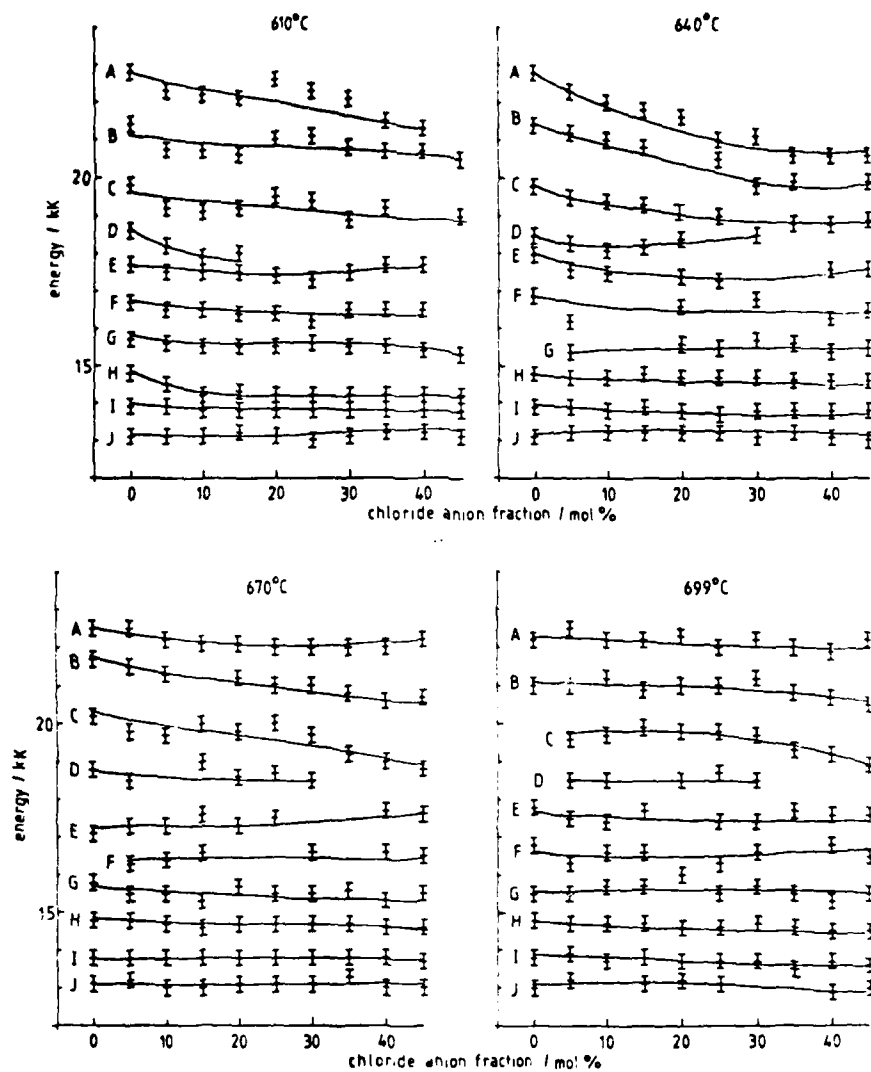chloride at 640°C. A. second derivative: B. fourth derivative.

Figure 9   Variation in energies of resolved bands of the chromium(III) spectrum in (Na.K.Al) (SO₄.Cl) with chloride content, at 610, 640, 670 and 699°C.

- 21 -

The marked absence of profile change with added chloride, and the lack of shift of the resolved bands, indicates clearly that only complexes of octahedral symmetry are to be found in these melts; the complex $[Cr(SO_4)_3]^{3-}$ is progressively changed to $[CrCl_6]^{3-}$.

The slow decomposition of these melts above 700°C suggests that the mechanism of Cr_2O_3 formation on the surface of chromium-containing alloys undergoing hot corrosion may well occur via the formation of an octahedral chromium(III) complex in the molten sulphate. Further work is needed in this area.

3.4. Iron(III) in Sulphate Melts with Added Chloride.

The spectrum of iron(III) in (Na, K, Al)SO_4 melt is dominated by a strong ligand-to-melt charge transfer edge, which completely swamps the weak, spin-forbidden $\underline{d}-\underline{d}$ transitions. The effect of chloride addition is to shift this edge progressively to lower energy (Fig.10).

An analysis of these spectra, including higher analyses, has been published as a preliminary communication (8). It was concluded that only tetrahedral sulphate complexes, probably $[Fe(SO_4)_4]^{5-}$, were present in the pure sulphate melt, and the addition of chloride caused the progressive replacement of sulphate ligands to form, ultimately, tetrahedral $[FeCl_4]^{-}$.

3.5. Isosbestic Points

An isosbestic point (and occasionally more than one) can sometimes be observed in a set of spectra where one parameter of the system is progressively varied: Fig.11 shows a stylised example. The presence of an isosbestic point is good evidence for the presence of two species in equilibrium in the system, their relative concentrations varying as the parameter is varied
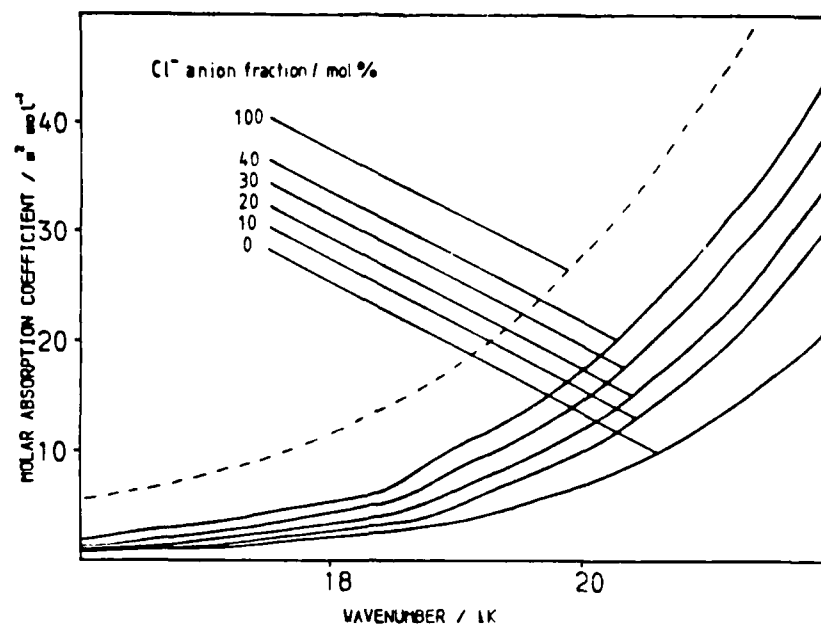
Figure 10   Variation of iron(III) spectrum in (Na,K,Al)(SO$_4$,Cl) with chloride content,
and spectrum in (Na,K,Al)Cl (dashed line), at 699°C (47 point smoothing,
fifth order polynomial).
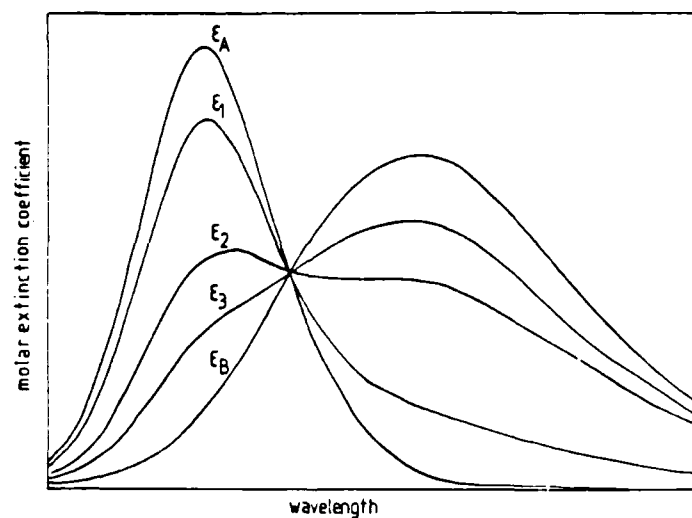
Figure 11   Stylised internally linear spectra of a two-species equilibrium,
A $\rightleftharpoons$ B. The spectra of A and B are plotted together with three
spectra of the equilibrium mixture, nominally recorded at three
different values of the external parameter.

(exceptions to this are specialised and rare). Fig. 1 shows the spectrum of nickel(II) in the (Na,K,Al)SO_4 eutectic melt as chloride is added, and added such that only the sulphate/chloride mole ratio is progressively varied, the cation ratios being maintained constant. Expressed in terms of mole per cent chloride added, it can be seen that isosbestic points appear over a limited chloride concentration range. By taking two spectra within this range as reference spectra it is possible (10) to generate the profile of any other spectrum recorded in this range (Fig.12). The procedure (10) may be extended to generate the spectra of the two individual species (Fig. 13) which, combined in varying ratios, produce the observed spectra. One of the individual species is identified as the octahedral nickel(I) complex ion $NiCl_2(SO_4)_x$, where x is probably 2 (i.e. the complex has two bidentate sulphate ligands), but it could be 3 or 4, the complex having two or four monodentate sulphate ligands. The other species is the tetrahedral nickel species $NiCl_3(SO_4)$.

It is thus possible to identify, and quantify, the individual species (corrosion products) within complex molten salt mixtures (simulating deposits).

4.   HOT CORROSION OF SUPERALLOYS

There are several superalloys in use in gas turbine engines, including IN 738, IN 716, IN 100, Hastalloy X, René 80 and René 95. Samples of all of these were obtained, the IN 738 from Dr. S.R.J. Saunders, National Physical Laboratory, London, and the rest from the Materials Section, Wright-Patterson AFB, Dayton, Ohio. Unfortunately the American samples did not arrive until the practical side of the contract was almost completed. Further, our Mechanical Workshops were unable to section them into the required dimensions. We were recently informed by Dr. M. Khobaib (Wright-Patterson AFB), when on a visit to England, that he had
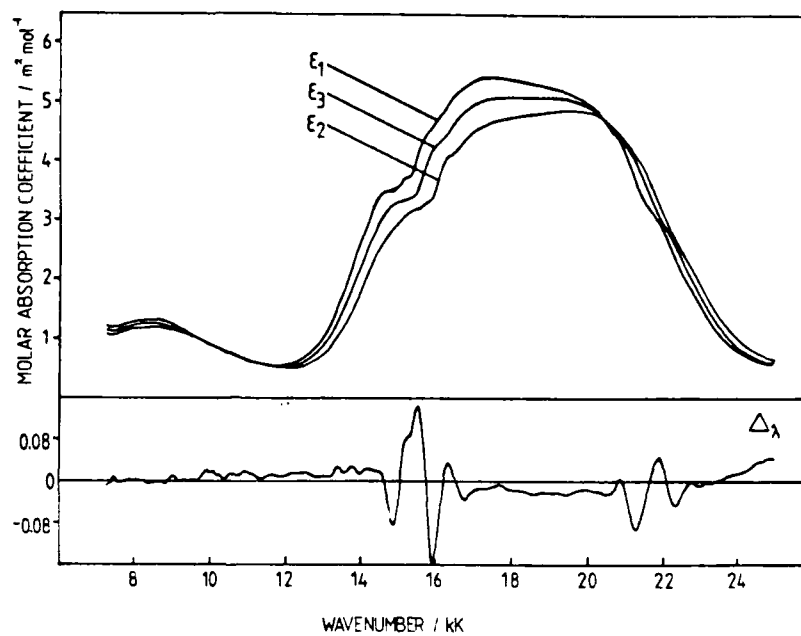
Figure 12   Internal linearity function, Δ_λ, for $\mathcal{E}_3$ (25% chloride), relative to $\mathcal{E}_1$ (30% chloride) and $\mathcal{E}_2$ (20% chloride), at 628°C.
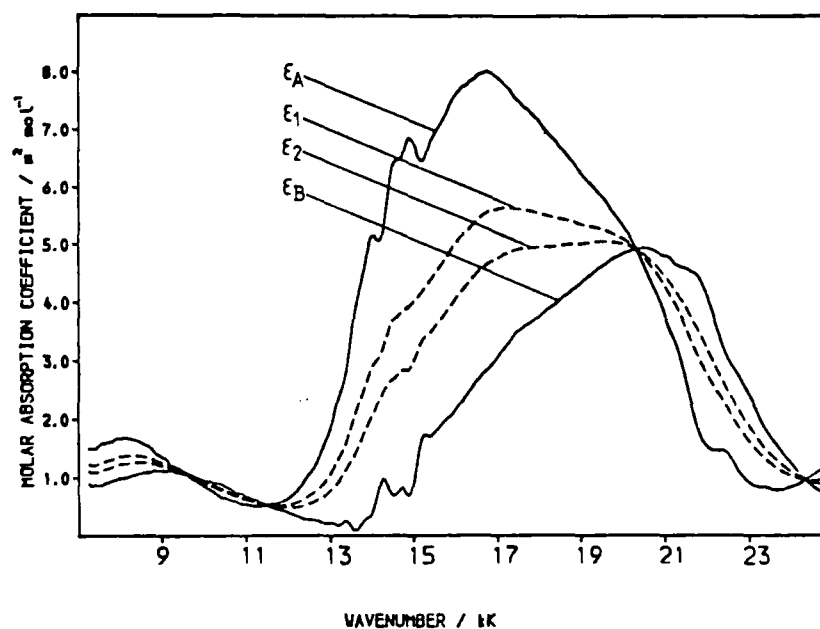
Figure 13   Terminal spectra, ε_A and ε_B generated from ε_1 (35% chloride) and ε_2 (25% chloride) at 587°C, with β_A = 2.98, and β_B = -2.70.

periodic access at WPAFB to the specialised equipment required,
and we have just received sections of suitable size of RENÉ 80.
So far, we have therefore had time to investigate only IN 738
samples, and we used both crucible tests and spectroscopic studies.

4.1. Crucible tests

A range of crucible tests were made on the superalloy IN 738.
Specimens were cut from rods designed and notched for use
in the carousel holder used in gas burner rig studies (at the
National Physical Laboratory). Half the specimens were polished
with Lindé alumina of various meshes on a Selvet cloth, and the
rest were oxidised by heating in air for 24h at around 620°C. The
melts chosen were pure sulphate, and sulphate with 20 mole per
cent chloride. The cations present were lithium, sodium and
potassium, and maintained at a ratio of 78 : 13.5 : 8.5,
respectively. Aluminium —containing melts were not utilised
since these experiments were long-term, and the volatile Al_2Cl_6
would be lost from the chloride-containing system. The tests were
further sub-divided into those conducted in air, with the remainder
under a synthetic combustion gas mixture containing SO_2 and SO_3.

Samples of the melts were taken at periodic intervals for
elemental analysis, and the maximum run was 262 h. Table 1
summarises the various conditions employed. The tests were
therefore continued for several days. In the early stages no
detectable coloration occurred. Later, in several cases, a grey
light cream coloured opaqueness appeared, but it was difficult to
conclude whether this was due to metal ions entering the melt, or
to precipitate oxides, or the effect of reflected light. After
about a week distinct colours could be seen in some crucibles,
ranging from blue to green, and some underlying greyness: a few
samples appeared pale yellow over the grey.

Quantitative determinations were made on melt samples for
the major component elements, namely, Ni, Co and Cr, and also for

Table 1.   Results of crucible tests of samples of IN 738 in molten

(Li, Na, K)SO$_4$ eutectic at 620°C.

A[a]	hrs	18	84	180	B	hrs	24	42	108	204
oxidised[b]	Fe	0.25	0.1	0.15	unpolished	Fe	0.25	0.2	0.1	0.7
sulphate[c]	Ni	N	T/N	0.1	sulphate	Ni	N	N	0.2	5.9

C	hrs	24	42	108	204
polished	Fe	0.2	0.2	0.1	0.2
sulphate	Ni	N	N	0.1	1.4

Pretreatment	Melt	hrs	Ni	Co	Cr
D unpolished	sulphate + 20% chloride	238	1.55	0.25	N
E polished	sulphate + 20% chloride	238	8.50	0.08	0.65
F oxidised	sulphate	192	0.40	0.02	N
G unpolished	sulphate	238	1.10	0.10	0.05
H polished	sulphate	238	0.25	0.01	N
J oxidised	sulphate + 20% chloride	192	0.75	0.10	0.45
K unpolished	sulphate	262	1.55	0.10	N
L polished	sulphate	262	0.05	0.05	0.08
M oxidised	sulphate	262	3.05	0.05	N

a, Specimen identifier

b, Nature of pre-treatment of specimen

c, Eutectic sulphate melt, containing Li, Na, K at 78:13.5:8.5 mole per cent

iron, which is present in IN 738 to < 0.5%. The melt samples, upon
solidification, were not completely soluble in distilled water; a
residue remained, and tests were therefore made on both parts.
Surprisingly no metal ions could be detected in the water soluble
portions. From the residues, after dissolution in acid, iron was
detected in the early stages (ca. 24 h) but did not subsequently
increase in concentration. Nickel was detectable after about 100 h,
and steadily increased in concentration, becoming the most abundant
species as expected. Cobalt was the next most abundant, followed by
chromium. Towards the end of the run their average detected
quantities, relative to chromium as unity, were : Co, 1.14 and Ni, 29.3.

It was clear from the results that the melts containing 20%
chloride attacked the samples approximately twice as fast as the
pure sulphate melts, but more data is needed to determine whether
there is a significant difference in the extent of attack on polished,
unpolished or oxidised samples.

Some melt samples were closely inspected under a microscope as
water was added. The purpose was to ascertain whether the greyish
coloration seen in the melt was due to metal ions entering the melt,
or small metal particles.

A dry fragment of the melt, around 1 mm diameter, was generally
observed as a mixture of forms and colours. These ranged from white
wisps on the surface and white crystalline blocks through to grey-
purple and dark grey-purple patches containing black dots and lines.
Upon addition of water the fragment dissolved and collapsed like a
sand castle, producing bubbles and breaking into granules of around
20 μm diameter. The granules had a distinct sard colour, and the
black particles had the look of metal inclusions from 50 μm down to
less than 1 μm in diameter. However, upon the addition of more
fresh water some of these darker fragments dissolved.

The tentative conclusions we can therefore reach at this time are that 260 h are insufficient for metal ions to enter the melt in sufficient concentrations to enable standard analytical techniques to detect them in the small melt samples removed, though they were later seen in our spectroscopic studies. Reactions may have taken place on the surface, and then particles flaked off and entered the melt. These particles cannot be flakes of the superalloy itself since the elemental ratios are different, viz., relative to chromium as unity the ratios are, for alloy and particle respectively, 3.86 and 29.3 for nickel and 0.52 and 1.14 for cobalt. There are therefore a considerable number of crucible related experiments and analyses required for a more complete understanding.

4.2 Spectroscopic Studies

Spectra were recorded of a (Li, Na, K)SO_4 melt containing a coupon of IN 738 over a period of thirteen days. An isothermal furnace was used, and the sulphate melt maintained at 700 ± 20°C and synthetic combustion gas containing SO_2 passed over the melt for the duration of the run. The sulphate powder, after melting, was held at temperature for about ten hours, during which time its spectrum against air was regularly recorded, to ascertain that no changes or decomposition were occurring. The specimen was then added and spectra recorded at regular intervals. At 117 h it was noted that no changes had been observed for some time and so pellets of (Li, Na, K)Cl were added to the melt to bring the chloride concentration up to 20 mole percent. Spectra were then taken almost continually and the run stopped after 303 h. After about 207 h some difficulties were encountered with the apparatus due to, it is believed, SO_3 in the combustion gas beginning to attack the plastic tubing and silicon rubber bung. Small dark particles were seen entering the melt, and causing a rising absorption throughout the spectral region. Though this was at this time essentially eliminated by baseline correction future long term experiments will be redesigned.

a. Spectroscopic Results.

Upon introduction of the metal specimen into the sulphate melt a slow rise in absorbance commenced, about 0.1 absorbance units in 16 h. (The specimens were first polished and then oxidised in air at 620°C for at least 24 h.) The absorbance decreased sharply for four hours, and then steadily for twenty hours, after which it remained essentially constant for fifty hours, but with a slight overall rise. On adding chloride (20 per cent) after 117 h a slow rise was seen for 18 h, after which it steadied off. Figure 14 shows some of the spectra obtained over this time span, and Figure 15 the combined results for several specimens at a fixed wavelength, as described above.

b. Computer Treatment of Spectra.

In an attempt to identify the ions entering solution derivative spectra were calculated: some examples, also showing computer plotted spectra, are given in Figures 16-19. Because the concentration of the ionic species in solution is here small the spectra had to be mathematically smoothed, to reduce noise contributions, but upon differentiation small narrow peaks appear more intense. We have catalogued the position of all the peaks that could be reliably identified, but upon comparison with peak maxima for nickel, chromium, cobalt and iron species were unable to identify unambiguously the presence of sulphato complexes of these elements. Complexes of the lesser components of IN 738 (Ti, 3.4; W, 2.55; Ta, 1.75; Mo,1.70 and Nb, 0.9%) may also have been contributing to the observed spectra, but we have not yet a sufficient spectroscopic data base to identify their presence, though work in this area has commenced in our laboratory.
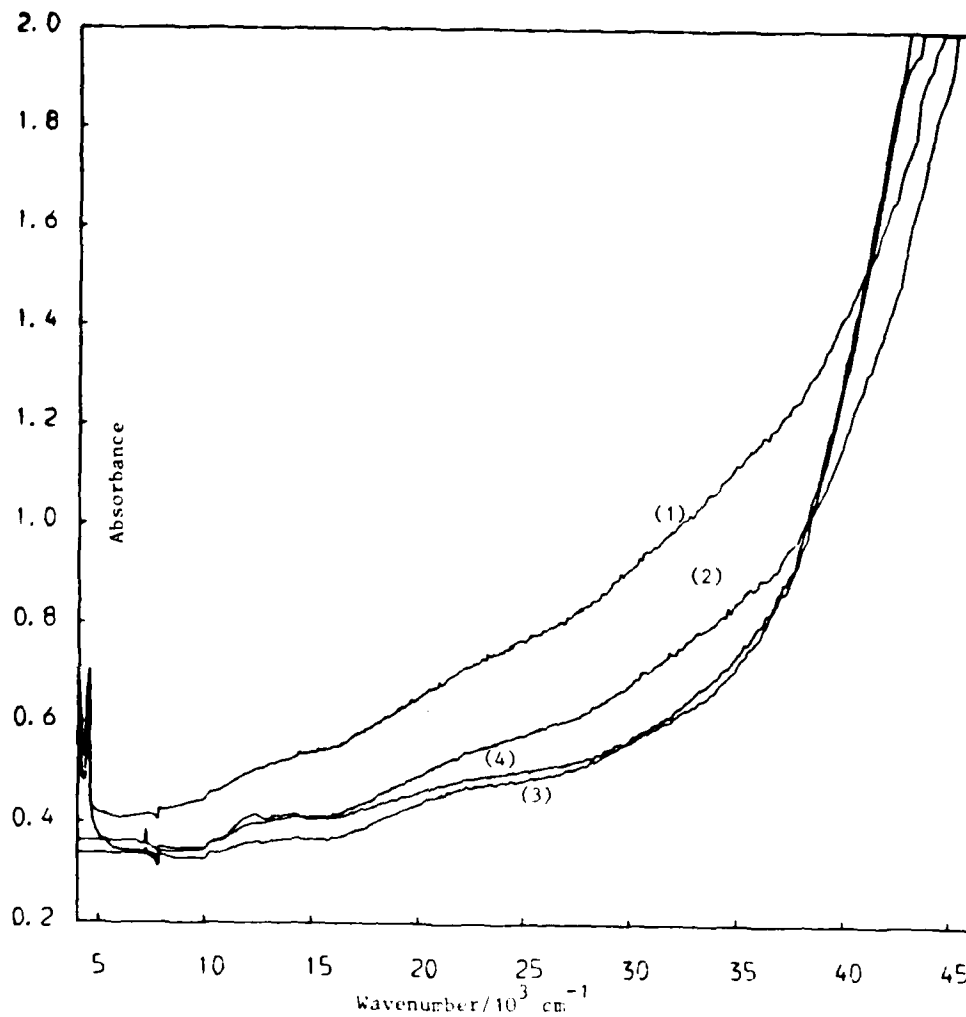
Figure 14. Examples of absorption spectra recorded of corrosion products formed in solution after various immersion times of a sample of IN 738 in molten (Li,Na,K)SO₄ eutectic at 700°C.

(1), after 24 hours; (2), after 43 hours; (3), after 117 hours; and (4), after 191 hours. Note that after spectrum (3) was recorded (Li,Na,K)Cl was added to give a chloride concentration of 20 mole per cent and thus spectrum (4) reveals chloride attack, by the appearance of dissolved corrosion products (probably chloro-sulphato transition metal complex ions) in the 7,000-25,000 cm^{-1} wavenumber region.
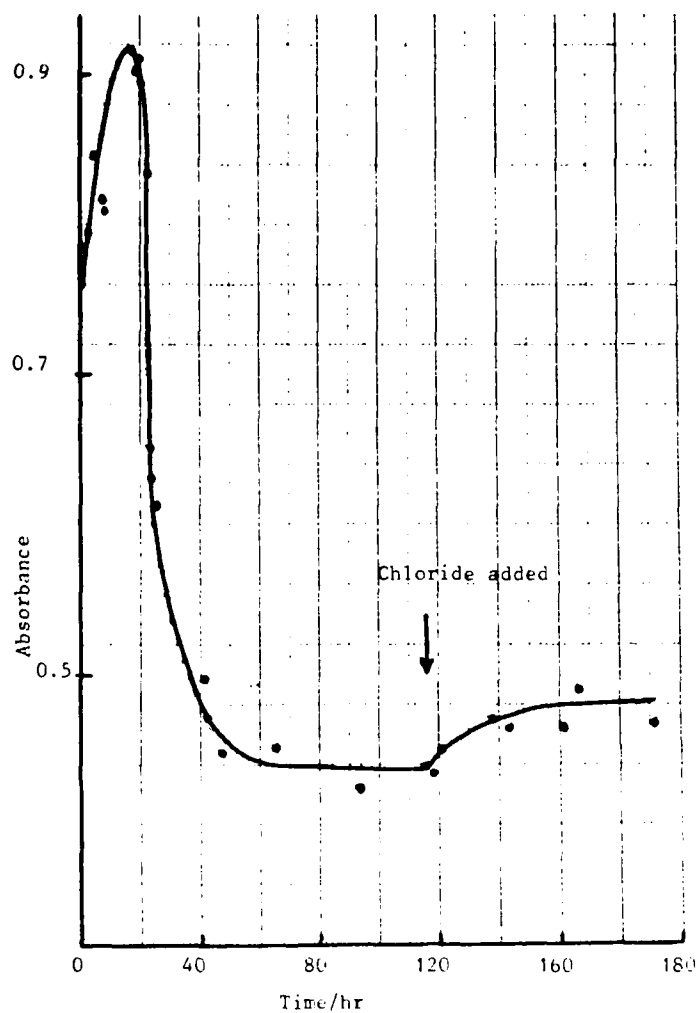
Figure 15. Variation in absorbance, at 500 nm, with time of corrosion products formed in a melt of (Li,Na,K)SO$_4$ eutectic at 700°C above a sample of IN 738. Arrow indicates time at which (Li,Na,K)Cl was added to give a chloride concentration of 20 mole per cent. Note that after the first few hours of initial reaction some corrosion products precipitate out and a plateau, probably a passive state is reached. Addition of chloride immediately causes attack of the passivated surface. Attack was more rapid if the IN 738 was placed initially in a chloride-containing melt.

- 33 -
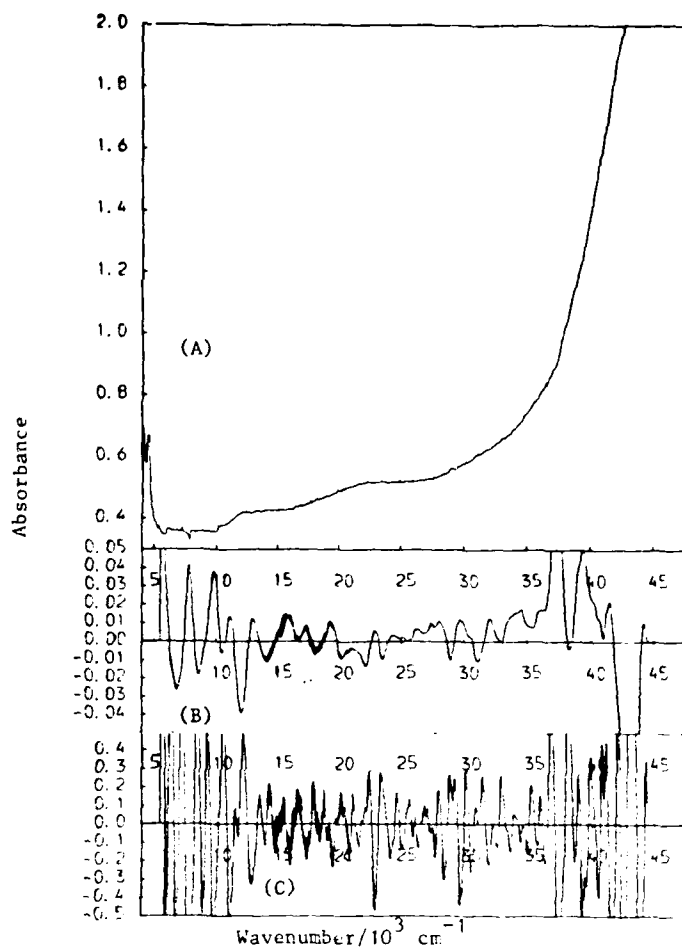
Figure 16. (A), Absorption spectrum of the corrosion products in a (Li,Na,K)SO$_4$ eutectic melt above a specimen of IN 738 after 116 hours immersion at 700°c.

Possible band maxima are identified by their computed second derivative minima (B), which correspond well, as expected, with their computed fourth derivative maxima (C).
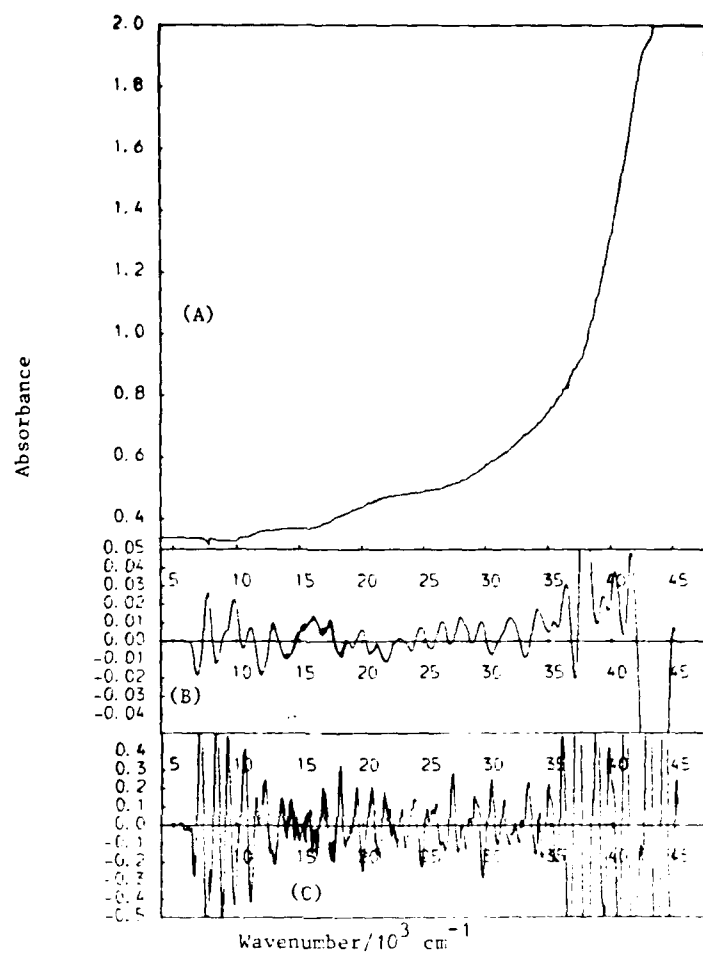
Figure 17. (A), Absorption spectrum at 700°C of the corrosion products from a specimen of IN 738 after 117 hrs in molten (Li,Na,K)SO$_4$ followed by 50 hrs after melt composition changed to SO$_4$: Cl of 80 : 20 mole per cent. (B) Second derivative and (C) fourth derivative spectra. Note increased band resolution in fourth derivative.
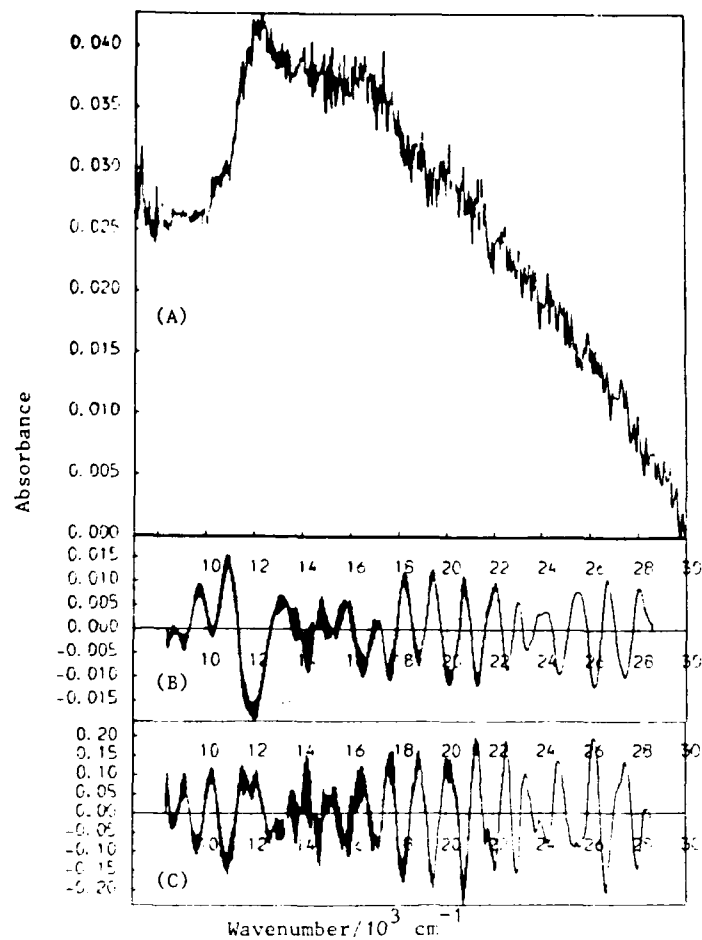
Figure 18. (A), Plot of difference spectrum between spectra (3) and (4) in Figure 14 showing net effect of chloride addition. (B) and (C) second and fourth derivatives, respectively. The parameters used in the mathematical computations were chosen so as to reveal the broad overall features of the constituent bands, viz., a 25 point convolute with a quadratic and quartic polynomial, respectively, with a sampling interval of 60 cm^{-1}.

Figure 19. (A), Plot of difference spectrum between spectra (3) and (4) in Figure 14, but the second (B) and fourth (C) derivative spectra have been calculated so as to reveal the finer features of the constituent bands, and thus enhance identification. Sampling interval now 40 cm^{-1}.

c. Present Conclusions

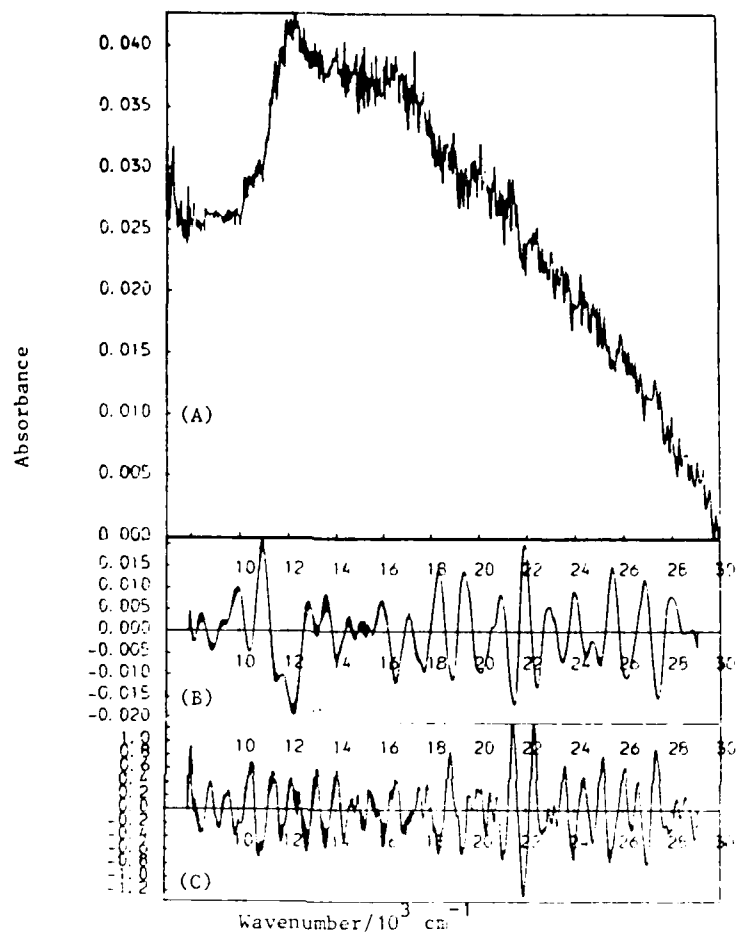The preliminary results show that during the first twenty hours of exposure of IN 738 samples to molten sulphate, transition metal ions enter the melt. Some of these then commence precipitation out of the melt as a result of reacting with (most probably) the oxide ions generated in the melt. The precipitate settles out in the melt, by gravity, adjacent to the sample. In addition, or alternatively, some of it may bond to the sample surface in the form of a scale, or a scale may form subsequently, or even independently, or after the surface of the sample is depleted of certain elements and a particular composition (range) is reached. Further experiments can resolve this.

The effect of introducing chloride at this stage is to increase slowly the concentration of transition metal ions in the melt, thereby indicating that the precipitate and/or the oxide layer formed on the surface is attacked by chloride: this is of course consistent with the general expectation of increased corrosion rates in the presence of chloride. The identities and concentrations of the ions formed in solution have not yet been determined, but this should be possible upon a combination of further crucible tests, n longer spectroscopic runs, computer treatment of spectra, and variation of the melt composition. Metallurgical tests on coupons with adherent melt, e.g. electron microprobe analysis (EMPA) would help confirm the results of such tests, and also identify the composition of adherent oxide or scale, and that of a possible layer in the melt (deposit) adjacent to the scale. One of the most significant findings in our studies on pure nickel, (3), (and indicated in incomplete work on iron and chromium samples (16)) has been the existence of a layer (0.2 mm approx. thick) in the melt,

---

(16). T.R. Griffiths, K. King and S.H. Marchant, unpublished results.

- 38 -

but adjacent to the scale, and that the rate determining step for, certainly nickel dissolution, is the transport of (nickel) ions through this layer. The presence of this layer in superalloy hot corrosion studies is therefore expected, and so far indicated by our results, and a major future task is to identify and measure it, and determine its role in the (slow) attack of molten sulphates (and chlorides) on superalloys. Its role, after several hundred hours exposure of superalloys to melts, to accelerated hot corrosion can also be studied.

5. RECOMMENDATIONS FOR FUTURE WORK

Our original Research Proposal outlined our aims and gave a statement of work for a three year period. We consider that the work described above, and in the Appendices, constitutes approximately the first third of the total work envisaged: it was initially stated that 'The first 12 months will be spent attuning the EASE technique to gas turbine corrosion, providing preliminary results, and establishing required fundamental information'. Our work on hot corrosion on superheater and reheater tubes in coal fired plant continues to be supported by the SERC and the CEGB, NE Region, (we have a research student for the next three years and some technical assistance). Thus continuation of this project will still have the benefit and resources of on-going research on the EASE technique and hot corrosion, and with much the same aims.

The recent workshop-conference on The Interaction of Molten Salts and Metals : Current Understanding of Hot Corrosion and New Approaches to Practical Problems (17) organised and edited by the Principal Investigator, is the latest and most complete survey and forward looking account of hot corrosion. It spans both the American and European views on the nature of molten salt attack and brought together for the first time molten salt chemists and specialists in hot corrosion, but trained in metallurgy and materials

---

(17) Proceedings of the Molten Salts Discussion Group Workshop—Conference on 'The Interaction of Molten Salts and Metals : Current Understanding of Hot corrosion and New Approaches to Practical Problems', 2-4 July 1986, University of York, sponsored by the Office of Naval Research US Navy, London Branch Office, edited by T.R. Griffiths, Hon. Secretary, Molten Salts Discussion Group.

science. This occasion enabled the latter to describe the problems encountered, and their materials solution, and the former to reflect thereon and offer information and approaches based on their understanding of molten salt chemistry and the behaviour of molten salt systems which, for example, contained species which could also be hot corrosion breakdown products. Thus it is particularly timely that the impetus started, and the international contacts gained, by this workshop-conference should be continued at the earliest possible opportunity. Also, it was stated in the original Research Proposal that a second spectrophotometer would be sought, and this has now been acquired, and will shortly be interfaced with a microprocessor and data capture and processing equipment.

The second twelve months of the Research Proposal were to be 'spent on fundamental and practical studies and on identifying corrosion mechanisms,' and this would be followed. It is recognised that, after the initial attack on superalloys, (which we have made preliminary investigations upon here with the EASE technique), subsequent (catastropic) attack occurs after long term exposure, often not before 2000 hr (around 80 days). We have therefore plans and prepared furnaces for such studies : samples of melt would be taken at regular intervals and examined spectroscopically and analytically for the appearance of corrosion products in the melts, at which time detailed EASE investigations would commence. Parallel metallurgical investigations would be made, utilising equipment available to us at Leeds, (and at times employing the specialised apparatus in the laboratories of the CEGB, NE Region in nearby Harrogate). Such combined studies on initial hot corrosion attack and the later catastropic (or accelerated) corrosion will yield new information on the mechanism of the latter, at present not understood. Further, it may indicate the possible role of initial attack on the timing and nature of later attack, and hence lead to recommendations for delaying the latter.

Additional fundamental studies are necessary, for monitoring
and determining the mechanisms of the initial attack, since so far
we have concentrated upon codifying the behaviour and spectra of
nickel, chromium and iron in molten salts : some studies on cobalt
are required, and no spectral studies have been reported for the
superalloy component elements, niobium, tantalum, molybdenum and
tungsten in sulphate melts. Since, for example, niobium metal
dissolves rapidly and dramatically in molten sulphates (18) it is
vital to identify the nature, and stability, of the chemical
species so formed in solution : our present studies on initial
attack on IN 738 have indicated weak bands in the spectra which
cannot as yet be fully identified, and it is possible that they
arise from species involving niobium and similar elements.

There are therefore many fruitful topics for study using spectral
and crucible measurements, and the EASE technique, all of which focus
on the hot corrosion products formed in the corrodant, a powerful
approach which yields mechanistic data and parallels and contributes
to metallurgical and electrochemical investigations. It is our
experience that those trained in these last two techniques are not
well versed in modern solution chemistry and theory, or the
interpretation of spectra : they are therefore (understandably)
reluctant to commit themselves and accept our claimes and findings.
The links must first be obvious. Our expanding contacts with this
community are clearly leading us to utilise a synthesis of techniques,
incorporating in particular electrochemistry, where simultaneous
spectroscopic and electrochemical measurements can be made. We
therefore, with further funding, would undertake a symbiotic
approach, spectroelectrochemistry of metals in melts, which without
doubt is needed, and will considerably clarify and enhance our
current understanding of the hot corrosion of turbine alloys.

---

(18). Private communication from Dr. J.E. Stringer, Electric Power
    Research Institute, Palo Alto, California, USA.

Appendix A

Thermal Gradient Furnaces.

A.1. Introduction

   We have already indicated that the EASE technique employs
spectroscopic measurements at various positions within a vertical
thermal gradient. Our publications on the technique (2,3) have
only included a cursory description of one of the furnaces we have
used and we therefore here give a more complete account.

   The design of the furnace is first described, then the
choice of optical system necessary to examine a thin horizontal
section of the silica cell containing the molten salt is discussed,
and finally, the effects of the optical modifications on the
spectrophotometer performance are examined.

A.2. Furnace design

   The principal feature of the various furnaces used is that
a pair of masks containing narrow, horizontal apertures remain
fixed in the light beam while the furnace is moved vertically, to
bring different sections of the melt into the light path created
by the aperture of the masks. (Fig. A1).

   The vertical cell housing and horizontal light ports of the
first furnace built (V, Fig. A2) were made of aluminous porcelain
tubing (id 4.5 cm, od 5.5 cm); the inner ends of the light port
tubes were cut to fit the curved surface of the vertical tube. The
Kanthal (12.6 Ω m^{-1}) heating element (C) was a uniform coil around
the outside of the vertical tube, with a spacing of 3 mm and a
total resistance of 100 Ω, and regulated by an Ether temperature
controller. The windings terminated just above the light port
tubes, giving a thermal gradient of around 30°C cm^{-1} in the cell
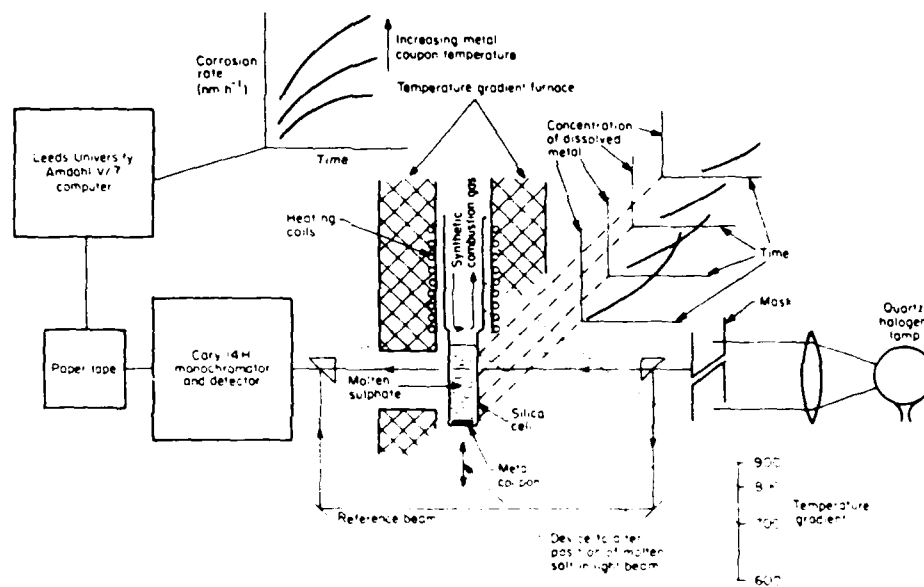space. The high temperature of the winding necessary to establish

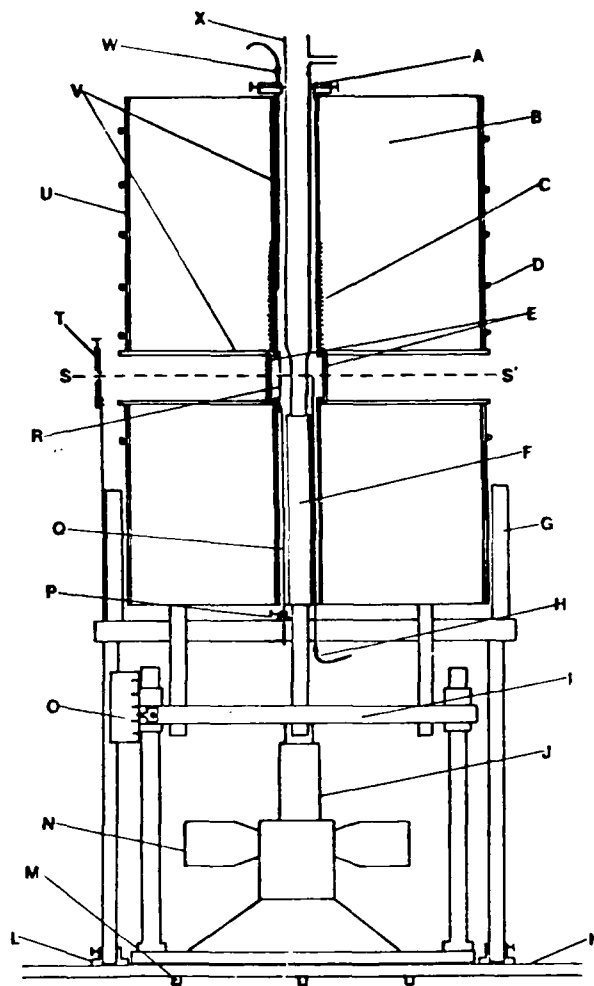Figure A.1. Schematic outline of the EASF technique.

Figure A 2 Thermal gradient furnace (legend on facing page)

- 44 -

sufficiently high temperatures in the cell space reduced the life of the heating element considerably. Frequent rewinding was necessary, and also time-consuming recalibration procedures. It was later found that the element life could be extended to more normal expectations by cementing the windings in place with ultra-pure cement.

The furnace assembly rests in the spectrophotometer cell compartment in a brass plate (K); the furnace is held in position by three locating lugs (M), while the table is held rigidly, and reproducibly, in the leg clamps (L).

The inner mask (R) is an interchangeable inconel screen, containing an aperture 8 mm wide, and mounted on a ceramic rod, which is fixed to the furnace table by a locking screw (P). Screens containing apertures of various heights were investigated. A second mask (T), having an aperture 8 mm wide and of variable height, was mounted at the light exit port.

The thermocouple (H), by Thermocoax, Philips, was used to measure the temperature of the horizontal section of melt being examined, and was also fixed to the table, with its tip in contact with the side of the silica cell, and in line with the apertures of the two masks. All three were adjusted to be in the vertical centre of the light beam. This thermocouple was calibrated using a second, identical thermocouple contained in a tight-fitting silica sheath, and immersed in a melt contained in a silica cell.

Different horizontal sections of the melt were brought into the aperture upon raising or lowering the furnace, using the graduated furnace position wheel (N). This controls the height of the platform (I) supporting the furnace via the 1mm pitch screw thread. The furnace position, and hence the sample position, was thus known to ± 0.005 mm and could be altered by very small increments.

A.3. Variable thermal gradients

The above furnace design, with a single heating element above the molten salt, gave essentially a constant temperature difference between the bottom of the silica cell, where the metal coupon was located, and the melt-gas interface near the top of the cell. In practice, this difference was around 100°C, and the synthetic combustion gas flowing over the melt passed through a zone of 800-900°C before reaching the melt-gas interface, which varied from about 680-730°C. It was considered important that the temperature gradient was capable of being varied independently of the melt-gas interface temperature.

A similar furnace was designed but with an independently controlled heating element below the silica cell. This furnace was not constructed in the Department's workshops, but to our design by Severn Science Ltd., Bristol. The upper heating wire was platinum and the lower was Kanthal. The furnace worked well, but the second heating element meant that the thermal gradient across the silica cell was no longer essentially linear. This also meant that the furnace calibration was a slow, time-consuming process.

The second variable thermal gradient furnace was later built in our workshops, with both sets of windings of Kanthal: the platinum upper winding of the Severn Science furnace was chosen partly so that much higher synthetic combustion gas and melt-gas interface temperatures could be investigated: unfortunately time did not permit this possible aspect of this project to be investigated beyond a few preliminary experiments.

Appendix B

Optical System

B.1. Spectrophotometer optical arrangement

The specialist optical system of the Cary 14H spectrophotometer is shown schematically in Fig. B1. This spectrophotometer was specifically designed so that accurate spectra can be obtained of samples that may be glowing white hot. Its essential feature is that its optics are reversed, so that the light beam is chopped before passing through the cell compartment and monochromator. By amplifying the AC (chopped) component of the AC and DC signal from the detectors (G, A), the spectrophotometer is able to eliminate photometric errors due to both stray light, and black body radiation from a hot sample (19), the latter producing the (continuous) DC detector signal.

The foci are also unusual in this instrument. Radiation from the light source (BB or CC) passes through the condensing lens (AA) to the beam splitter (Z). The focussing mirrors (DD,DD') form the image of the horizontal aperture at the chopper (X). The image of the vertical aperture is focussed at the screens (Y, and Y'). The focussing elements (W and W') give images of the vertical slit at (U) and (U'), while the image of the vertical aperture is formed at (T) and (T'); the image of the horizontal aperture is at infinity. The distance S-U, S'-U' is 20 cm, and this section is shown in detail in Fig. B2.

After passing through the cell space, the beams are recombined (Q) and directed through the slit (P) to the double monochromator comprising the grating (N) and a prism (J) in series. The light is finally brought to the appropriate detector (A or G).

(19). D.M. Gruen, Quart. Rev. Chem. Soc., 1965, 19, 349.

Key to Figure

BB.CC: light sources

AA: condensing lens

Z: beam splitter

DD.DD': focussing mirrors

YY': screens

X: chopper

W.W': focussing elements

EE EE': mirrors

U.U': image of vertical slit

T.T': horizontal slit image

S.S': image of vertical aperture

Q: beam combiner

P': cylindrical lens

P.L.H: monochromator slit system

O.M: grating colimator mirrors

N: grating

K.I: prism colimator mirrors

J: prism

E: movable mirror

D.B: focussing lenses

C: flat mirror

F: focussing element
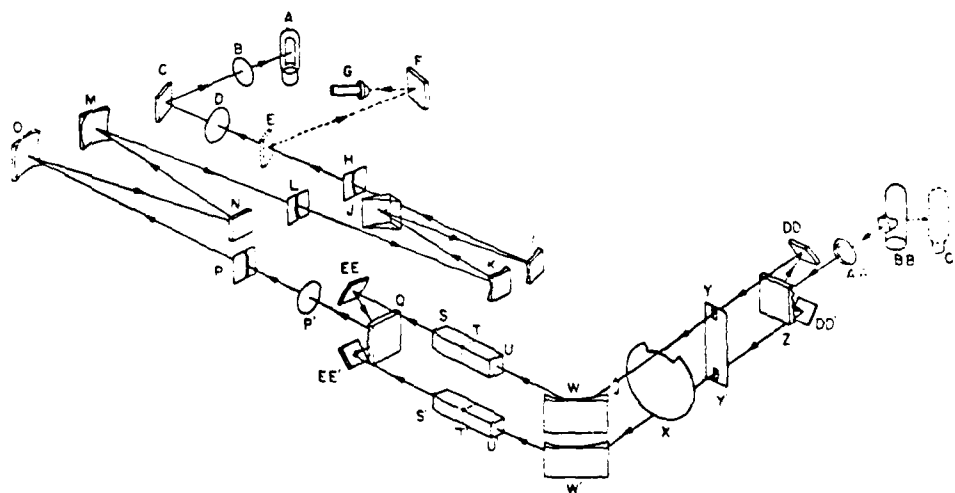
G: PbS detector

A: phototube detector

Figure 81 Optical arrangement of the Cary 14H spectrophotometer reproduced by courtesy of Varian Ltd
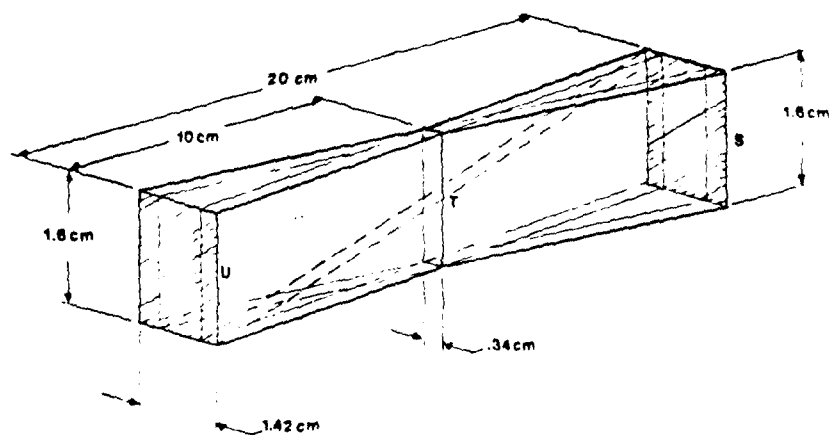
Figure B 2 Optics in cell space. S vertical aperture image; T, horizontal slit image; U vertical slit image (the horizontal aperture image is at infinity).

In practice, however, the two light beams do not behave in the cell compartment as expected, because the quartz-halogen lamp employed is a non-point source. As a result, the light passing through the sample is no longer parallel in the vertical plane. This is because each of the many point sources of the tungsten filament gives rise to a set of rays behaving ideally, but no two sets of rays will be parallel and the resultant of their combination is a slightly divergent beam passing through the sample.

This means that the positions of the interposed masks in this particular application become critical. With a beam parallel in the vertical plane, a mask inserted at any position along the light path will sample the same section of the cell, having the dimensions of the aperture in the mask. This is no longer the case with non-parallel light, and it was therefore necessary to establish the sampling characteristics of various mask configurations in order to select the most suitable combination.

B.2. Selection of Optimum Mask System

A photographic step plate (Kodak Ltd., London) was chosen to simulate a non-uniform concentration gradient. The tablet was a piece of photographic negative, 22 mm x 33 mm, having horizontal steps, 3 mm wide, of increasingly greater absorbance. The range of absorbance was from 0.05 to 3.05, in eleven steps of nominal absorbance increment of 0.3.

The tablet was centrally mounted on the cell location platform, so that raising the furnace would alter the observed absorbance in a stepwise fashion. The ability of a chosen mask system to cut out light from all but a thin horizontal section of the tablet would then be evident from the degree of 'stepping' in a plot of absorbance _versus_ furnace position.

Nine possible mask configurations, designated (i) - (ix), were examined (Table B1). For each combination the absorbance

Table B1. Various mask combinations examined

System	Inner mask Aperture height/mm	Outer mask Aperture height/mm
(i)	1	1
(ii)	1	2
(iii)	1	3
(iv)	1	removed
(v)	2	2
(vi)	2	3
(vii)	2	removed
(viii)	removed	1
(ix)	removed	2

was recorded at 0.5 mm vertical intervals from the clear section of the tablet, below the first step, to the seventh step. Various calibrated neutral density screens brought the absorbance readings on scale. This was carried out, for each mask combination, at three representative wavelenths, viz., 400, 800 and 1200 nm.

The results showed a clear division between combinations (i) - (iv) and (v) - (ix). The latter showed only slight undulations in the plots of absorbance versus furnace position, indicating that a relatively large section of the tablet is sampled with such combinations. A representative plot, for system (vi), is shown in Fig. B3. Conversely, systems (i) - (iv) gave plots with well-defined steps, typified by that for system (iii) in Fig. B4.

Configurations (v) - (ix) were clearly inadequate for sampling narrow, horizontal sections in the cell space, and were therefore discarded. To establish which of the configurations (i) - (iv) gave the narrowest sample section, the slopes of the nominally horizontal parts of the steps were calculated, and are shown in Table B2. The thinnest sample sections are indicated by the smallest slopes. The results show that the effect of increasing the outer mask aperture height from 1 mm (system (i)) to 2 mm (system (ii)), while the inner aperture height remains at 1mm, is quite small. Greater increases in slope are apparent on going from 2 to 3 mm outer aperture height, and when removing the outer mask completely.

Clearly, the optimum system would have been that in which both inner and outer masks had aperture heights of 1mm (system (i)). However, because of its high initial absorbance, this system would be limited to samples with maximum absorbance around unity. For this reason, and also because the change on going from system (i) to system (ii) is small, it was decided to use system (ii), i.e.,

Figure B 3   Variation of observed step tablet absorbance with
furnace position for mask configuration (vi).
A. 400 nm; B. 800 nm; C. 1200 nm (curves offset
for clarity).

- 53 -
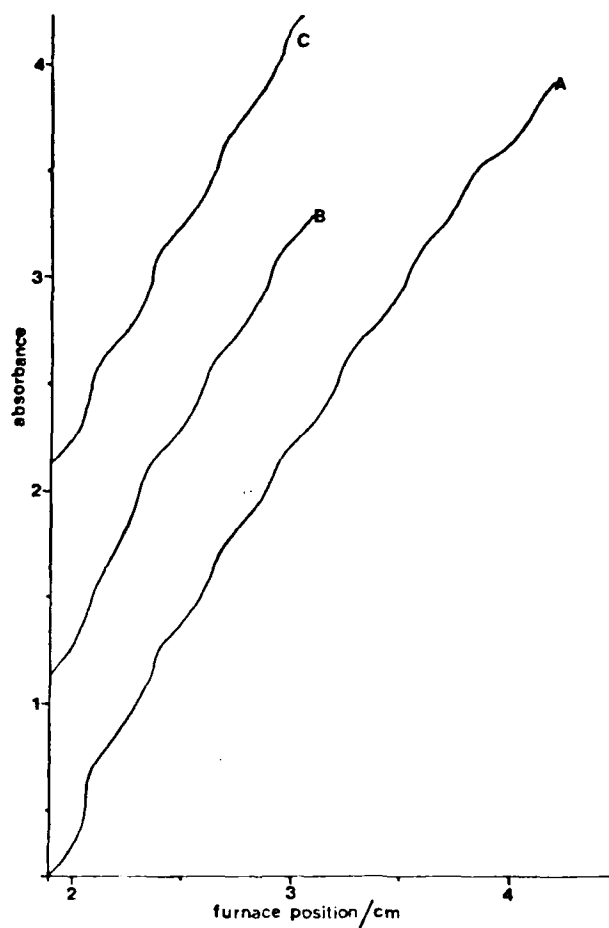
Figure B4   Variation of observed step tablet absorbance with
furnace position for mask configuration (111).
A. 400 nm; B. 800 nm; C 1200 nm (curves offset
for clarity).
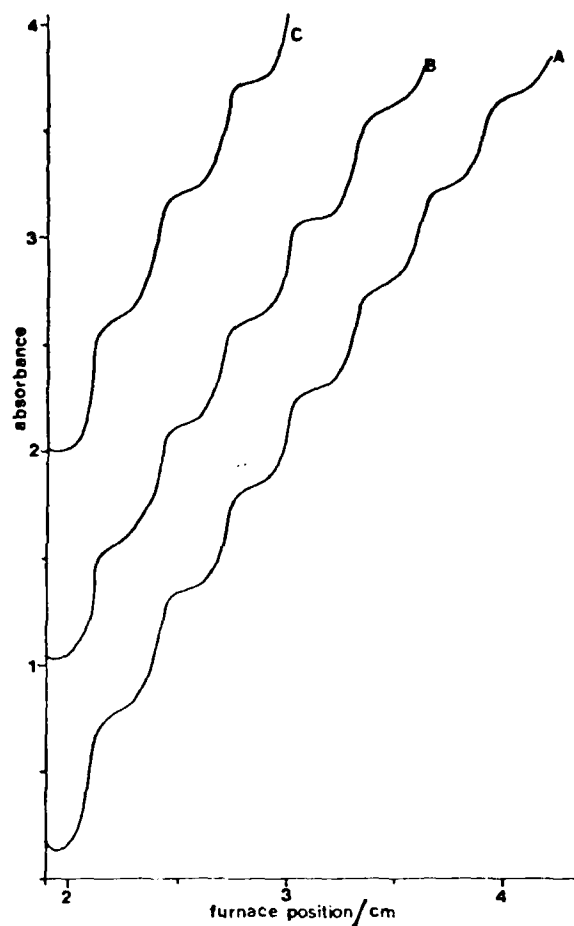
- 54 -

Table B.2.   Gradients of lines fitted to steps from absorbance
plots for systems (i) - (iv)

System	Wavelength /nm	Slope of line fitted to step $(\times 10^3)$					
		2	3	4	5	6	7
(i)	400	39.4	40.2	18.8	26.6	33.4	–
	800	33.6	36.0	–	–	–	–
	1200	43.6	31.2	–	–	–	–
(ii)	400	35.2	44.0	27.4	36.0	39.4	27.6
	800	36.4	35.6	26.4	40.4	–	–
	1200	37.2	35.4	32.8	29.2	–	–
(iii)	400	44.0	55.4	38.2	60.0	44.4	51.8
	800	39.0	39.4	20.0	72.0	–	–
	1200	44.4	32.4	37.6	58.6	–	–
(iv)	400	59.8	62.8	58.0	69.8	51.2	49.4
	800	55.2	94.6	43.4	45.4	85.6	–
	1200	63.2	63.0	56.6	76.4	74.6	–

inner mask aperture 8 mm x 1 mm, and outer mask aperture 8 mm x
2 mm, for this study. The next stage is to establish the dimensions
of the melt section which is sampled by this system, when the
melt is contained in the 10 mm square modified optical cells
(Fig. B5).

B.3. Size of Section Examined

To determine the height of the tablet being examined at any
one time, the section of the absorbance curve at 400 nm, spanning
tablet steps 2 and 3, was remeasured at 0.1 mm vertical furnace
movement increments. From this the position of the step boundary,
b, was accurately obtained, together with the actual absorbances,
A_2, A_3, of the two steps. These values were 25.8 cm, and 0.965
and 1.445, respectively. From these three parameters the expected
curves were calculated for various values of a variable, y, which
represents the actual height (above the base-plate) of the section
of tablet being examined. The method is as follows (with reference
to Fig. B6).

For the section of curve under examination there will be
three different expressions for the absorbance, A, depending upon
the furnace position, p; the actual sample height, y; and the
position of the step boundary, b, viz.,

(a)   if $p \leqslant b - (y/2)$, then $A = A_2$, where A_2 is the absorbance
of step 2;

(b)   if $p \geqslant b + (y/2)$, then $A = A_3$, where A_3 is the absorbance
of step 3; and

(c)   if $b - (y/2) < p < b + (y/2)$, when the absorbance will be
a combination of proportions of A_2 and A_3.

To obtain an expression for A within condition (c) consider
the absorbance at a position p' (Fig. B6), which will be given by

SYNTHETIC
FLUE
GAS
INLET

GAS
OUTLET

PLATINIZED
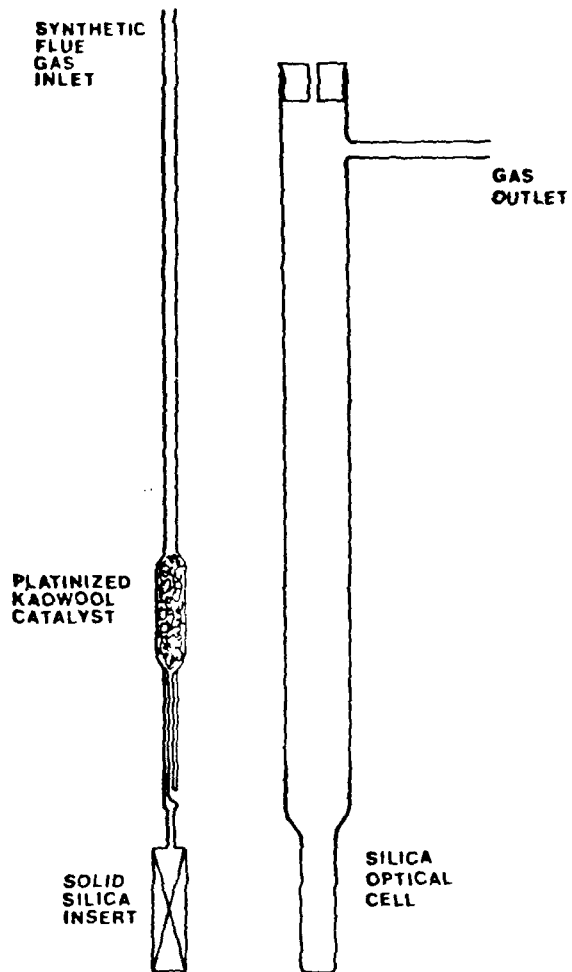KAOWOOL
CATALYST

SOLID
SILICA
INSERT

SILICA
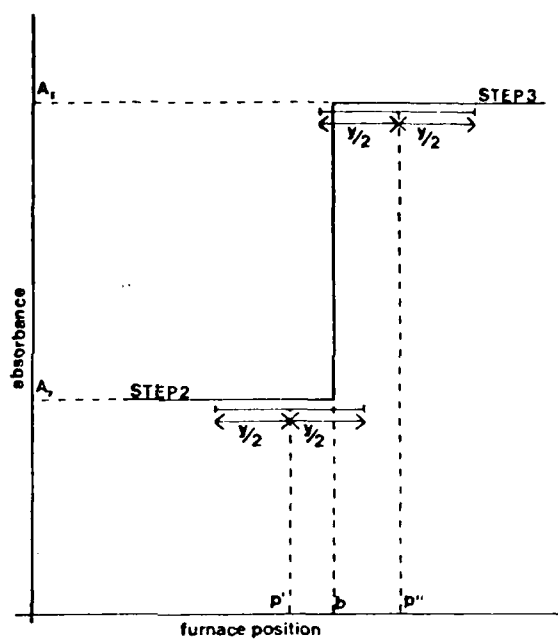OPTICAL
CELL

Figure B5   A modified optical cell and insert.

Figure 56 Calculation of theoretical curve
between steps 2 and 3, in terms of y,
the height of tablet section examined

$A' = [(y/2)A_2 + (b-p')A_2 + (p'+(y/2)-b)A_3]/y$. Similarly, at p'', the absorbance is given by $A' = [(y/2)A_3+(p''-b)A_3 + (b-(p''-(y/2))A_2)]/y$

These expressions are equivalent, and can be simplified by replacing $(y/2)$ by α and $(b-p)$ by β, to give one expression for the absorbance for condition (c), namely,

$A = [(1+\beta/\alpha)A_2 + (1-\beta/\alpha)A_3]/2$

This equation was used to calculate the lines shown in Fig. B7. It can be seen that the best approximation to the observed curve is obtained with y in the region 1.4 - 1.6 mm.

The variation of the sample height across a cell of path length 10 mm was obtained from a scaled geometric drawing. If the height at the centre is taken as 1.5 mm, the corresponding maximum heights of the sample at the two optical faces of the cell are 1.25 and 1.75 mm. Since, in this particular application, very small increments in the change of furnace position were not required, a maximum light section height of 2 mm was assumed. Thus increments of 2 mm or more ensured that no overlap of examined sections of the specimen occurred.
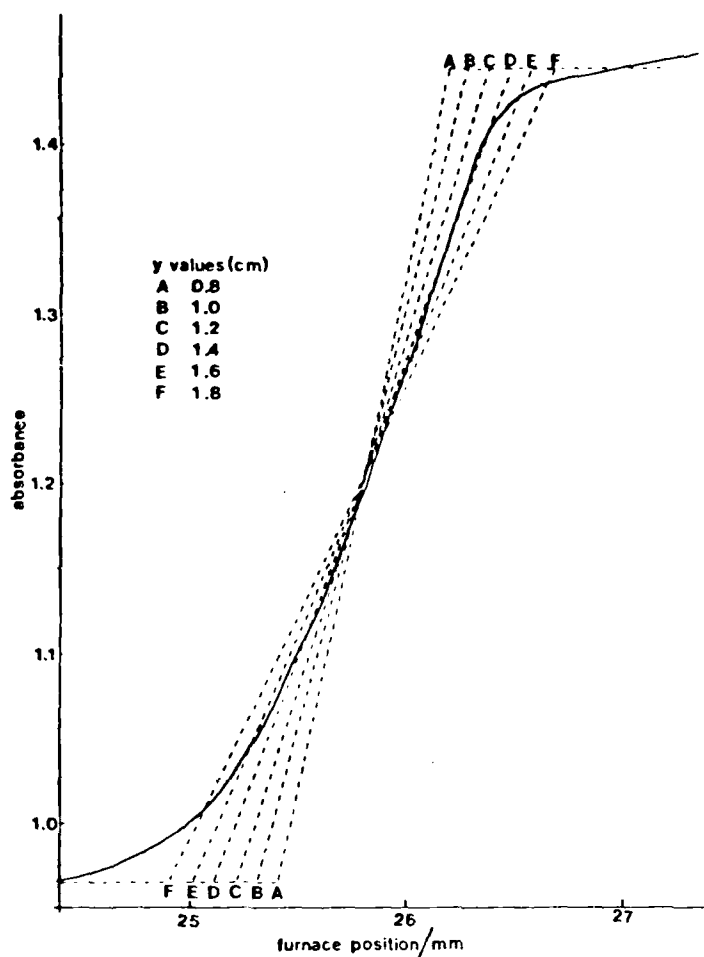
Figure B7 Actual curve (solid) and calculated lines (dashed)
for various values of y.

Appendix C

The Measurement of Accurate Spectra

The effect of masking all but a thin horizontal section of
the sample beam (and the consequent attenuation of the reference
beam) on the major features of spectrophotometer performance are
now discussed.

C.1. Resolution

The resolving power of the instrument is determined by the
spectral band width (SBW): the greater the spectral band width,
the poorer the resolving power. The spectral band width is given
by (20)

$$SBW = (D \times SW) + SCM + DL$$

where D is the reciprocal linear dispersion, SW the mechanical
slit width, SCM the slit curvature mismatch, and DL the diffraction
limit.

The contribution of both diffraction and slit curvature are
very small, and may be regarded as negligible for normal slit width
readings (20). Thus the mechanical slit width has the major
influence on resolution.

The slit servo-mechanism of the Cary 14H spectrophotometer
operates to maintain constant energy at the detector. The use of
neutral density screens on the reference beam will thus increase
the mechanical slit width, and hence the spectral band width. The
energy reaching the detector is proportional to the square of the
mechanical slit width. Hence, if a neutral density screen of

(20). Cary Instruments (Applied Physics Corporation, now Varian
      Instruments), Report AR14-2 (September, 1964).

- 61 -

transmission T% is placed in the reference beam, the slit width increases by a factor of $(100/T)^{\frac{1}{2}}$, to maintain a constant energy flux at the detector. Using the above equation, it is possible to calculate the various spectral band widths for different neutral density screens. The results, derived from data given in ref. 20 are presented in Table C.1. Screen combinations of the order of 6-8% T are typical in this application, and the resolving power will thus be reduced by a factor of three. However, this is much smaller than the variation in resolving power over the range 1400 - 400 nm when no neutral density screens are used.

C.2. Band Shape

The influence of the spectral band width on observed band shapes depends on the natural band width (NBW) of the peak under investigation. The optimum spectral band width is such that (20)

$\qquad$ (SBW)/(NBW) $\leqslant$ 0.1

and under these conditions the observed and true heights differ by less than 0.5%. The $\underline{d}$ - $\underline{d}$ bands recorded in this project have natural band widths in the range 100 - 200 nm; thus a spectral band width no greater than 10 nm will satisfy the above equation. In the wavelength range of interest (1400 - 260 nm) the spectral band width is greatest at 800 nm, and for a neutral density screen of 8% transmission has the value 3.29 nm (Table B3). Reducing the transmission to 1% gives a spectral band width of 9.0 nm. Therefore screen combinations having a resultant transmission of greater than 1% (i.e., an absorbance of 2.0) may be used without increasing the spectral band width above the optimum value.

In practice, screens have an absorbance of 1.2 - 1.4 units were used, and thus no distortion of peak height is expected.

•

Table C.1. Values of the spectral band width (nm) for different
neutral density screens in the reference beam.

Wavelength /nm	Percentage transmission of screen				
	100*	50	40	26	8
400	0.085	0.103	0.112	0.127	0.199
600	0.089	0.104	0.113	0.128	0.188
800	1.010	1.388	1.532	1.874	3.293
1000	0.590	0.076	0.851	1.022	1.730
1200	0.712	0.928	1.015	1.213	2.035
1400	1.011	1.334	1.463	1.760	2.987

* i.e. no screen

C.3. Signal-to-Noise Ratio

As previously stated, the Cary 14H spectrophotometer operates
with a constant reference signal at the detector. In the ultra-
violet and visible regions the detector employed is a photomultiplier.
With a photoelectric device such as this, the limiting signal-to-noise
(S/N) ratio is determined (21) by the 'shot noise', i.e. statistical
fluctuations in the signal arising from the nature of the processes
involved. The shot noise is proportional to the signal intensity,
and since this is kept constant, the absolute noise output of
the photomultiplier is fixed. The S/N ratio thus decreases in
proportion to the reduction in signal intensity from the sample beam.

In the infrared region the detector is a photoconductive (PbS)
device. In this case, noise is independent of light changes, and
again, S/N ratio will decrease directly with beam intensity.

In practice, the increase in pen noise has not been found to be
serious: it is taken into account when considering the photometric
error limits.

C.4. Stray light

Strictly, the term 'stray light' refers to stray radiant
energy (SRE). This is light resulting from imperfections in the
optics, and is outside the spectral band defined by the monochromator.
(The term is also often used to refer to background room light or
black body radiation from a hot sample; the elimination of these
effects has already been described.)

In the absence of stray radiant energy, the absorbance is
given by $A = \log(I_o/I)$, where I_o is the incident radiation, and

---

(21)   R.P. Bauman, 'Absorption Spectroscopy', John Wiley, New York, 1962.

I the transmitted radiation. With stray light contributing
equally to sample and reference beams (as it must do in the Cary
14H spectrophotometer optical arrangement), the observed
absorbance is $A_{obs} = \log[(I_o + SRE)/(I + SRE)]$. The SRE is
measured as a proportion of the flux leaving the monochromator,
and 0.001% is a reasonable figure for the Cary 14H. The optical
modifications applied will reduce both I_o and I, and hence also
the absolute amount of SRE. There will thus be no deviation in
the observed absorbance, and the spectra obtained in the project
are instrumentally reliable: errors which might arise due to
sample handling, etc., are discussed elsewhere in this report.

REFERENCES

1. T.R. Griffiths and K. King, J. Chem. Soc., Faraday Trans. 1, 1981, 77, 2763.

2. T.R. Griffiths, K. King and D. Mortimer, High Temperature Technology, 1982, 1, 43.

3. T.R. Griffiths, K. King and D. Mortimer, Power Ind. Res., 1982, 2, 79.

4. K.E. Johnson, R. Palmer and T.S. Piper, Spectrochim. Acta, 1965, 21, 1697.

5. G. Harrington and B.R. Sundheim, Ann. N.Y. Acad. Sci., 1960, 79, 950.

6. D.M. Gruen and R.L. McBeth, Paper for the Seventh International Conference on Coordination Chemistry, Stockholm (June 1962).

7. N.W. Silcox and H.M. Haendler, J. Phys. Chem., 1960, 64, 303.

8. T.R. Griffiths and K. King, Chem. Comm., 1981, 518.

9. J. Brynestad, C.R. Boston and G.P. Smith, J. Chem. Phys., 1967, 47, 3179.

10. T.R. Griffiths and P.J. Potts, Inorg. Chem., 1975, 14, 1039.

11. K.E. Johnson and T.S. Piper, Discuss. Faraday Soc., 1961, 32, 32.

12. G.P. Smith, in 'Molten Salt Chemistry', Ed. M. Blander, Wiley and Sons (1964).

13. T.R. Griffiths, K. King, H.V. St.A. Hubbard, M-J Schwing-Weill and J. Meullemeestre, Anal. Chim. Acta., 1982, 143, 163.

14. K.E. Johnson, Electrochim. Acta, 1966, 11, 129.

15. C.A. Angell and D.M. Gruen, J. Phys. Chem., 1966, 70, 1601.

16. T.R. Griffiths, K. King and S.H. Marchant, unpublished results.

17. Proceedings of the Molten Salts Discussion Group Workshop-Conference on 'The Interaction of Molten Salts and Metals : Current Understanding of Hot Corrosion and New Approaches to Practical Problems', 2-4 July 1986, University of York, sponsored by the Office of Naval Research, US Navy, London

Branch Office, edited by T.R. Griffiths, Hon. Secretary, Molten Salts Discussion Group.

18. Private communication from Dr. J.E. Stringer, Electric Power Research Institute, Palo Alto, California, USA.

19. D.M. Gruen, Quart. Rev. Chem. Soc., 1965, $\underline{19}$, 349.

20. Cary Instruments (Applied Physics Corporation, now Varian Instruments), Report AR14-2 (September, 1964).

21. R.P. Bauman, 'Absorption Spectroscopy', John Wiley, New York, 1962.

END

DATE
FILMED

3-88

DTIC